C.P. No. 1323

PROCUREMENT EXECUTIVE, MINISTRY OF DEFENCE

AERONAUTICAL RESEARCH COUNCIL

CURRENT PAPERS

Developments in the Lifting Surface Theory Treatment of Symmetric Planforms with a Leading Edge Crank in Subsonic Flow

-by-

B.L. Hewitt and W. Kellaway

LONDON: HER MAJESTY'S STATIONERY OFFICE

1975

PRICE £2 NET

CP No.1323*
October 1972

DEVELOPMENTS IN THE LIFTING SURFACE THEORY TREATMENT OF SYMMETRIC PLANFORMS WITH A LEADING EDGE CRANK IN SUBSONIC FLOW

- by -
B.L. Hewitt and W. Kellaway

SUMMARY

An attempt has been made to develop a subsonic lifting surface theory method capable of calculating convergent loading solutions for symmetric planforms with a leading edge crank. This document traces the time history of thought and method development at B.A.C. (Military Aircraft Division) which connects the successful treatments of regular and cropped delta type planforms that are reported in References 1 and 13, respectively. Finally, some mention is made of possible future generalisations of the basic cranked planform method.

CONTENTS/

---

*Replaces A.R.C.33 412

CONTENTS

CONTENTS (Contd.)

1. INTRODUCTION

Three-dimensional linearised theory contributes significantly in the subsonic design of lifting wings. Within the linearised theory framework, one of the main problems is the accurate evaluation of the improper double-integral associated with subsonic lifting surface theory. Reference 1 (1967) presented a critical survey of the then existing methods for solving the classical lifting surface problem and a brief account of the method developed at B.A.C. (M.A.D.).

The B.A.C. method, which is described in detail in Reference 2, has been shown to produce solutions to the classical lifting surface problem that exhibit excellent convergence characteristics. However, in common with the other methods described in Reference 1, the B.A.C. method is only applicable to "regular planforms"; i.e. planforms without slope discontinuities of leading and/or trailing edges. There was a definite requirement for a proper treatment of irregular, or cranked, planforms since they are of the type usually considered in practical wing design procedures.

This long standing practical requirement prompted B.A.C. to concentrate some thought and effort into an attempt to develop a lifting surface theory method capable of evaluating convergent loading solutions for cranked planforms. This document is intended to record the train of events which eventually led to the development of such a method, for a restricted class of planforms.

The work was carried out at B.A.C. (M.A.D) under research contract KD/3D/24 for the Aircraft Research Branch of the Ministry of Aviation Supply.

2. THE BASIC PROBLEM AND METHOD OF SOLUTION FOR REGULAR PLANFORMS

The basic integral equation of subsonic lifting surface theory may be written in the form

$$\frac{W}{U}(x_r,y_s) = -\frac{1}{8\pi}\iint_S \Delta Cp(x,y)\left[1 - \frac{(x-x_r)}{\{(x-x_r)^2+\beta^2(y-y_s)^2\}^{\frac{1}{2}}}\right]\frac{dx\,dy}{(y-y_s)^2}, \qquad (1$$

where $\frac{W}{U}$ is the local downwash or incidence distribution,

ΔCp is the unknown load distribution, and S is the planform area.

2.1 Regular Planform Methods

For planforms without cranks, termed regular planforms, several methods exist for the solution of (1), a few of which are outlined in Reference 1. The various methods may be segregated into groups such that each group contains methods having a number of common features. In general though all the methods embody the use of similar integration coordinates and loading representations.

Normalised variables are introduced such that

$$\eta = \frac{y}{s} \quad \text{and} \quad \xi = \left\{\frac{x-x_{\ell}(\eta)}{c(\eta)}\right\} , \tag{2}$$

so that the planform is transformed into the rectangle $\{-1 \leq \eta \leq 1, 0 \leq \xi \leq 1\}$,

n.b. it is assumed here that the planform is symmetric about $y = 0$ although asymmetric configurations can easily be catered for.

The loading distribution is approximated by means of an expression of the type

$$\Delta Cp(x,y) = \sqrt{1-\eta^2}\sqrt{\frac{1-\xi}{\xi}} \sum_{i=0}^{n-1}\sum_{j=0}^{m-1} a_{ij}\, P_i(\xi)Q_j(\eta) , \tag{3}$$

where $P_i(\xi)$, $Q_j(\eta)$ are usually chosen from known sets of orthogonal polynomials and the coefficients a_{ij} are unknown.

The problem is thus reduced to evaluating the mn unknowns a_{ij} by satisfying equation (1) at mn suitably chosen collocation points (x_r, y_s). The main numerical difficulties arise in evaluating the double integral in (1) for each of the terms in (3).

The essential difference between the B.A.C. method and all the other methods is that in the B.A.C. method the finite-part integration with respect to η along lines of constant ξ is performed first. Thus (1) is written in the form

$$\frac{W}{U}(\xi_r,\eta_s) = -\frac{1}{8\pi}\sum_{i=0}^{n-1}\sum_{j=0}^{m-1} a_{ij}\, W_{ij}(\xi_r,\eta_s) , \tag{4}$$

with

$$W_{ij}(\xi_r,\eta_s) = \int_0^1 P_i(\xi)\sqrt{\frac{1-\xi}{\xi}} \int_{-1}^{1} Q_j(\eta)\frac{c(\eta)}{s}\sqrt{1-\eta^2}\left[1-\frac{X}{R}\right]\frac{d\eta\, d\xi}{(\eta-\eta_s)^2} , \tag{5}$$

and

$$X = (x-x_r) , \quad R = \{X^2+\beta^2(y-y_s)^2\}^{\frac{1}{2}}.$$

The advantages of this procedure over those used in other known methods are described in Reference 1. The essential achievements are that calculation accuracy is unimpaired as collocation points approach edges of the planform and that no restrictions are imposed on positioning the points. In general, excellent convergence characteristics are obtained as the number of loading terms in (3) is increased.

At this point it is worth mentioning that the following general procedure has been advantageously followed at B.A.C. with respect to choosing and using integration coordinates in lifting surface theory problems.

(A) Use matched asymptotic expansion techniques to determine ΔC_p singularity orders and locations compatible with the required boundary conditions.

(B) Choose a pair of basic integration coordinates such that the ΔC_p singularity locations are exactly described within the families of coordinate lines. In general, the lines in a coordinate family should be smooth and regular although special points may be present at which derivative singularities need to be accommodated.

(C) Initial integrations should, if possible, be carried out with respect to a coordinate whose lines do not pass through the location of an infinite ΔC_p singularity.

In the present section, emphasis has been placed on the treatment of lifting surface theory problems related to smoothly distorted surfaces with regular planforms. For such problems, the ξ,η coordinates defined in (2) have already been extensively used by other workers in the field and they are also seen to satisfy the requirements made in (B). However, nearly all methods for evaluating the double integral of lifting surface theory involve an initial integration with respect to ξ, and this gives rise to severe numerical inaccuracy when evaluating the downwash at points close to the leading edge. The root cause of this trouble is located in the fact that the infinite ΔC_p singularity along the planform's leading edge is included in the first integration. This produces singular effects in the final integrand which become more and more difficult to handle as downwash points approach the leading edge. Incidentally, the same type of problem appears when use is made of any other initial integration coordinate whose lines cross the leading edge (see eg. Reference 3). All such methods are seen to violate the requirement in (C).

Less obvious examples of the value of using (A), (B) and (C) are to be found in the successful treatments of wings with control surfaces reported in Reference 4, and wings with a leading edge crank as reported in this document.

3. THE TREATMENT OF PLANFORMS WITH EDGE CRANKS

The direct application of the methods referred to in Section 2 to planforms with edge cranks would seem obviously doomed to failure, since the choices of coordinates and loading form made in (2) and (3) lead to logarithmically infinite downwash (i.e. $\frac{w}{U}$) values on the planform along each streamwise line through an edge crank.

With this in mind, some effort was made at B.A.C. to devise ways of overcoming the rather special mathematical problems associated with a lifting surface theory treatment of cranked planforms. In the following, a brief time-history is presented of the relevant thought development and measures adopted.

3.1 The Method Outlined in References 1 and 5

The first approach to be investigated involved the following simple reasoning. For symmetric planforms with edge cranks at the centre-line (i.e. $y = \eta = 0$), physical requirements are that $\Delta C_p(x,y)$ is smoothly varying and $\frac{d\Delta C_p}{dy} = 0$ at $y = 0$. In terms of the ξ,η coordinates of (2), these requirements infer that $\left(\frac{\partial \Delta C_p}{\partial \eta}\right)_\xi$ must be discontinuous across $\eta = 0$. Thus, if a separated form for ΔC_p is required, one is led to postulate that a plausible modification to (3) is gained by simply replacing η by $|\eta|$. Obviously, in general, the downwash contributions associated with the separate a_{ij} terms will contain logarithmic type singularities at $\eta = 0$. It is therefore necessary that the coefficients of these singularities reduce to zero when the contributions are added together. Analysis was used to extract the analytic expressions which define the downwash logarithmic singularity coefficients for each of the (i,j) loading terms. Equating the sum of the coefficients to zero was shown to be equivalent to requiring that the sidewash should be zero along $\eta = 0$; which is of course physically required. Thus it was possible to infer that convergent solutions for the a_{ij} might be found by using a collocation procedure which incorporates the zero sidewash condition at the wing centre-line. The main numerical problem lay in implementing this condition effectively, since it could only be imposed at a finite number of chordwise points. However, during the same period of time attention was turned towards some previous, little known work by Germain[6] and Legendre[7] on incompressible cross-flow around an infinite angular sector. Since, through the concepts of matched asymptotic expansions, the 'inner' problem of finding the linearised theory cross-flow potential in the neighbourhood of a cranked wing apex is exactly that investigated by Germain and Legendre, it was decided to redirect effort onto a practical assessment of their infinite sector work.

3.2 The Infinite Sector Solution and its Implications

Germain[6] showed that the problem of finding the linearised perturbation velocity potential, ϕ, around a plane infinite angular sector inclined to a free stream of speed U at an angle α has a set

of eigensolutions of the form

$$_i\phi = U \alpha r^{\nu_i} . f_i \left(\frac{y}{x}, \frac{z}{x}\right) \qquad i = 0(1)\infty$$

where r is the radius length from the apex given by

$$r^2 = x^2 + y^2 + z^2 \quad \text{(see Figure 1).}$$

Here, ν_i and f_i are the eigenvalues and eigenfunctions, respectively, and both are parametric functions of sector half angle γ.

Germain also showed that there is just one eigenvalue, say ν_0, in the interval (0,1) for all γ. This eigenvalue is such that

$$\nu_0 = \tfrac{1}{2} \quad \text{for} \quad \gamma = \frac{\pi}{2} \text{ (straight leading edge)}$$

$$\text{and} \quad \nu_0 = 1 \quad \text{for} \quad \gamma = 0 \text{ (slender-body theory approximation)}$$

Following on from Germain's work, Legendre[7] introduced the coordinates (r,θ,τ) such that

$$x = \frac{r \cos\theta}{\cosh\tau}, \quad y = \frac{r \sin\theta}{\cosh\tau}, \quad z = r \tanh\tau$$

and showed that the f_i satisfy the equation

$$\frac{\partial^2 f_i}{\partial\tau^2} + \frac{\partial^2 f_i}{\partial\theta^2} + \frac{\nu_i(\nu_i+1)}{\cosh^2\tau} \cdot f_i = 0 \qquad (6)$$

Then, through use of the conformal transformation

$$a + ib = \log\left(\frac{e^{\tau+i\theta} - e^{i\gamma}}{e^{\tau+i\theta} - e^{-i\gamma}}\right) - i\gamma \quad ,$$

he obtained the first two terms in series expansions for ν_0 and f_0 which are valid for small γ.

Using Legendre's work as a basis, analysis in Reference 8 shows that, across the sector in z = 0, the potential difference associated with the first eigenvalue problem may be written as

$$\frac{\Delta_0\phi}{U\alpha} \propto r^{\nu_0} u^{\frac{1}{2}} E_0(u;\gamma) \qquad (7)$$

where $u = \frac{(\cos\theta - \cos y)}{(1 - \cos y \cos\theta)}$ so that $0 < u < 1$ for $y > |\theta| > 0$

and where $E_o(u;y)$ is a regular function of u.

Using (7), the associated linearised form for ΔC_p may be written as

$$\Delta C_p = \frac{-2}{U\alpha} \cdot \frac{\partial \Delta_o \phi}{\partial x} \propto r^{\nu_o - 1} \cdot u^{-\frac{1}{2}} \cdot F_o(u;y) \qquad (8)$$

where F_o is a regular function of u, the proportionality indicating a degree of arbitrariness.

The form for Δ_ϕ given in (7) may be taken to represent the 'inner' solution associated with the apex neighbourhood of wings with a leading edge crank of half angle y. This should closely approximate the local variation of a 'fully matched' or 'overall planform' solution for any finite wing containing a similar leading edge crank. It was thought worthwhile to attempt to test the practical validity of such a concept by using (7) in conjunction with the 'regular planform' lifting surface theory method of Reference 2.

3.2.1 An attempt to gain numerical evidence from which to assess the practical value of the infinite sector solution

In Reference 9 a variety of convergence tests were carried out using the method of Reference 2. One of these tests involved the use of standard Multhopp-type collocation point distributions in attempting to gain convergence on a constant chord wing whose hyperbolic edges have a very small radius of curvature at the centre line. The exercise showed that ΔC_p convergence is very slow as the number of collocation points is increased. This ΔC_p convergence problem was found to be related to a large amplitude variation of downwash between collocation points, especially near the wing centre line. This is indicative that, in terms of the coordinates used in (3), the basic mathematical model requires a rapid variation of ΔC_p in the centre line neighbourhood and, because of the smooth global variation of the form assumed for ΔC_p together with the locally sparse spanwise distribution of boundary conditions (i.e. collocation stations), this requirement is only being met in a very approximate fashion.

Based on this evidence and reasoning, it appeared clear that the only effective way to improve overall convergence characteristics on wings with local rapid changes of edge curvature would be to modify the assumed form for ΔC_p. However, it also seemed possible that, using the original form for ΔC_p, a local improvement of solution quality might be gained by concentrating more boundary conditions in the relevant neighbourhood. Such a local improvement could be envisaged only at the expense of solution quality elsewhere on the wing.

A test of the truth of this conjecture is reported in Reference 9 where solutions for the aforementioned hyperbolic edged wing, using full-span Multhopp collocation distributions on each half wing, are discussed. This unusual type of collocation distribution concentrates boundary conditions near the centre line as well as near the tips. It was found that solution convergence characteristics near the centre line are greatly improved but those further outboard are drastically worsened.

This positive result led to calculating so-called 'Half span Multhopp' solutions for the artificially rounded planform illustrated in Figure 2a. In the centre line region plots were made of $\log\left(\frac{\Delta\phi}{U\alpha}\right)$ as a function of $\log r$ along lines of constant θ, where r and θ are measured with respect to a displaced cartesian system with origin at the pseudo crank apex (see Figure 2a). These plots are illustrated in Figure 3 and, through use of limited range least squares fitting techniques, it was shown that the family of lines could be represented by $\log\left(\frac{\Delta\phi}{U\alpha}\right) = \bar{\nu} \log r + \log D(\theta;\gamma)$

$$\text{or} \quad \frac{\Delta\phi}{U\alpha} = r^{\bar{\nu}} \cdot D(\theta;\gamma) \quad \text{for } 0 < |\theta| < \gamma$$

where $\gamma = \frac{\pi}{4}$, $\bar{\nu} = 0.816$ and $D(\theta;\gamma)$ is the function illustrated in Figure 4. The symmetric nature of D together with its singular behaviour near $\theta = \pm\gamma$ allowed it to be rewritten as

$$D(\theta) = u^{\frac{1}{2}} \cdot \bar{E}(u;\gamma), \text{ where } \bar{E} \text{ is regular near } \theta = \pm\gamma,$$

so that $$\frac{\Delta\phi}{U\alpha} = r^{\bar{\nu}} \cdot u^{\frac{1}{2}} \cdot \bar{E}(u;\gamma)$$

which is now in the infinite sector form given by (7); $\bar{\nu}$ and $\bar{E}$ can thus be thought of as approximations to ν_0 and E_0, respectively.

Work on the fundamental eigenvalue problem has been carried on by a number of different workers. Brown and Stewartson[10] derived asymptotic expansions for ν_0, valid near $\gamma = 0$ and $\frac{\pi}{2}$, and refined their estimate of ν_0 for $\gamma = \frac{\pi}{4}$ through a numerical procedure. Starting from Legendre's equation for the f_i (see (6)) and using finite difference techniques, Rossiter[11] gained numerical solutions for the mixed boundary value problems in terms of the unknown parameters ν_i. This formulation finally led to evaluating the ν_i through solving a matrix eigenvalue problem.

For $\gamma = \frac{\pi}{4}$, the available best estimates for ν_0 are:

Brown and Stewartson	:	0.8147
Rossiter	:	0.8145

and these are to be compared with the approximate value of 0.816 gained from the currently reported work at B.A.C.

Recent work by Taylor[12] has provided an accurate expansion for the function $F_0(u;\frac{\pi}{4})$ where F_0 appears in the expression

$$\frac{F_0(u;\frac{\pi}{4})}{F_0(1;\frac{\pi}{4})}$$

for ΔC_p given by (8). A comparison of values for this function from Taylor's expansion and from the B.A.C. results is illustrated in Figure 5. The agreement is seen to be remarkably good, especially considering the exploratory nature of the B.A.C. work.

Thus for a finite planform with small radius of curvature rounding of the leading edge (see Figure 2a), the evidence strongly suggests that near the pseudo apex the behaviour of the solution is of the geometrically related infinite sector type. This correlation necessarily breaks down in the immediate neighbourhood of the locally rounded edge.

As has already been inferred in Reference 9, this locally valid infinite sector behaviour of $\Delta\phi$ may be expected near all leading edge cranks irrespective of orientation of the line of symmetry. A special case of a leading edge crank is found at the forward tip corners of a wing with finite tip chord. From solutions using a standard Multhopp type of collocation point distribution it has been found that $\Delta\phi$ is indeed symmetric about the bisector of the tip corner angle and that its local variation along lines of constant θ (see Figure 2b) may again be accurately represented by (7).

Having collected evidence to show that the infinite sector solution may be regarded as a locally valid 'inner' solution for finite wings, the problem remained of how to use this information in formulating the lifting surface theory problem such that it converges to the required 'fully matched' solution.

3.3 A Discussion of Different Approaches to Finding 'Fully Matched' Linearised Solutions for Wings with a Leading Edge Centre-Section Crank

In tackling lifting surface theory problems through the use of 'inner' solution information it is sometimes possible to split the solution process into the following three main steps.

Step one involves using explicit 'inner' solutions in choosing a suitable non-arbitrary form for a 'partially matched' loading. Step two uses information gained from step one in defining a subsidiary lifting surface problem of a type already known to be soluble. Finally, a converged solution of this subsidiary problem is combined with the loading chosen in step one to give a 'fully matched' solution to the original problem. An example of such a procedure is to be found in the treatment of wings with control surfaces reported in Reference 4.

However, when attempting to use the infinite sector solution in treating planforms with edge cranks this approach cannot be used as it stands. A possible variation on the theme might be to generalise the B.A.C. procedure already described in Section 3.2.1. This would involve developing a lifting surface theory method suitable for a convergent treatment of planforms with locally rapid radius of curvature variations, and then using the arbitrariness in the infinite sector form in (8) to attempt to effect a good matching of solutions.

A more direct approach may be initiated through making a careful choice of a suitably arbitrary representation for the 'fully matched' loading. The necessary arbitrariness in the representation may be thought of, in general, as requiring that the loading be expressed in terms of a weighted sum of two-dimensional modes. This set of modes may contain subsets each of which corresponds to a different area of influence.

Through the lifting surface theory integral equation each loading mode gives rise to a two-dimensional downwash mode whose shape characteristics depend, not only on the chosen loading mode, but also on the shape of the geometric area over which the double-integral is evaluated. The degree of success in solving a specific boundary value problem thus depends on how convergent are combinations of these downwash modes in fitting the required normal velocity distribution over the specified planform area. If one considers only the simple case of simulating smooth imposed downwash variations, then due care should be exercised to ensure that the chosen set of loading modes does not contain anomalous members which require irregular or near irregular variations in their corresponding downwash modes. Incidentally, it is often found convenient to assume that the two-dimensional loading variations may be expressed in terms of separated one-dimensional modes, as has been done in (3).

Such reasoning indicated that a number of choices of loading representation might be suitable for treating the current problem. These choices were divided into two main categories, each of which will now be discussed.

3.3.1 Loading Representation by Means of Local or Regional Modes

The concept of local modes becomes useful if the planform area is divided up into two or more adjoining regions and it is required to separately represent the loading over each region.

The main problem associated with such a representation lies in choosing the regional modes such that a sufficient degree of continuity is maintained across region boundaries. If this is not done adequately then the corresponding downwash modes will exhibit singular variations at the boundaries and doubt is cast on the validity of any resulting loading solutions. Examples of this type of representation are to be found in the 'overlapped patching' techniques mentioned in Reference 8, and in so-called 'panel methods'.

'Overlapped patching' was an attempt to satisfy continuity requirements by forcing modes associated with any one region to terminate with polynomial type zeros along lines inside the adjacent regions. Thus, modes associated with any two adjacent regions overlap in the neighbourhood of the common region boundary, and the degree of continuity along the terminal lines may be adjusted through choice of the order of polynomial zeros. However, a one-dimensional numerical exercise showed that this forced termination of the loading modes introduces downwash mode variations which are extremely rapid near the terminal points, thus leading to an ill-conditioned problem.

On the other hand, 'panel methods' have been, and are being successfully employed in treating non-linear problems through the use of surface singularities. However, at the time that the currently outlined work sequence was in progress, it was felt that linearised lifting surface theory required a degree of loading continuity across panel boundaries which might make the application of panel methods to such problems impracticable.

3.3.2 Loading Representation by Means of Global Modes

The term global modes is used to infer that the range of applicability of such modes is restricted only by the planform boundary. Since such modes extend over the complete planform it is prudent to couch them in terms of coordinates which have been chosen to satisfy the requirements in (B) of Section 2.1.

In what follows, discussion will be restricted to the treatment of planforms whose leading edges are cranked at the centreline (η=0) and may be described by

$$x = x_{\ell}(\eta) = |\eta| . f(\eta^2) \qquad (9)$$

where f may only be irregular at η=1, or

$$\eta = \eta_{\ell}(x) = x . g(x) \qquad (10)$$

where g is regular. The planforms are also assumed to have regular trailing edges of the form

$$x = x_t(\eta) = h(\eta^2) \ . \qquad (11)$$

Examples of such planforms are illustrated in Figures 6a and b. At B.A.C., the development of ideas related to a choice of global representation suitable for planforms of the above type took place in two distinct phases, and these will now be discussed.

Phase I: The Global Representation of Reference 8

As indicated in Section 2.1, an initial consideration in treating all lifting surface theory problems is concerned with the choice of coordinates with which to work. Although due attention was paid to the requirements in (B) of Section 2.1, it was thought advantageous to also bear in mind the conical nature of the loading in the neighbourhood of the crank apex. This resulted in advocating the use of the coordinates ζ and χ defined by

$$\zeta = \eta/\eta_{\ell}$$

and $$\chi = x/x_t \quad ,$$

where η_{ℓ} and x_t are of the forms given in (10) and (11), respectively.

In the ζ,χ plane, the planform thus becomes the rectangle given by $-1 < \zeta < 1$, $0 < \chi < 1$. Typical coordinate lines are illustrated in Figure 6a and the pseudo conical form of those for constant ζ is clearly seen. Using these coordinates and the 'inner' solution form given in (8), it was thought that a suitable 'fully matched' global representation for the loading could be written as

$$\Delta C_p = \chi^{\nu_0 - 1} \cdot \sqrt{\frac{1-\chi}{1-\zeta^2}} \sum_{i=0}^{\infty} \sum_{j=0}^{\infty} a_{ij}\, T_i(2\chi-1) T_{2j}(\zeta)$$

where $T_n(u)$ is a Chebyshev polynomial of order n with $-1 < u < 1$.

Also, in an attempt to satisfy the requirement stated in (C) of Section 2.1, it was decided to integrate initially with respect to χ along lines of ζ.

However, as may be seen from Figure 6a, there exists a region forward of the trailing edge in which the form of the ζ coordinate lines is such that they tend to become parallel to lines of constant η. This property of the ζ coordinate lines, together with the non-linear relation giving η in terms of ζ and χ were found to introduce severe numerical integration problems and inaccuracies for the following reasons.

The kernel function of the integral equation contains an improper singularity having the cartesian form $(\eta-\eta_s)^{-2}$. An initial integration with respect to χ thus produces singular effects in the ζ plane which are very difficult to identify in an analytic fashion. This difficulty is most severe for integration along lines which become nearly parallel to the stream direction in the vicinity of $\eta = \eta_s$. The consequence of not having an accurate analytic description of the ζ plane singularities is that it is impossible to gain accurate downwash values from the second integration. It was thus decided that the approach was impracticable and the phase of work was therefore discontinued.

Phase 2: The Global Representation used in Reference 13

Work during Phase I showed that severe numerical integration difficulties were introduced by using coordinates which pandered to the conical form of the 'inner' solution. Most of these difficulties stemmed from transforming the improper cartesian singularity in the kernel function, and this therefore suggested that η should be selected as one integration coordinate. Having made this choice an attempt was then made to choose a second coordinate subject to the requirements of (B) in Section 2.1.

Referring to (2), the coordinate ξ, which is introduced for regular planforms, is seen to satisfy the requirements of (B) for cranked planforms except that the coordinate lines are cranked also. Thus for cranked planforms, from the definition

$$x = x_\ell(\eta) + \{x_t(\eta) - x_\ell(\eta)\}\,\xi \quad ,$$

the lines of constant ξ are seen to possess discontinuous slope with respect to η corresponding to the discontinuous slope of $x_\ell(\eta)$. However, for planforms with leading and trailing edges of the form of (9) and (11), respectively, an analogous coordinate to that of (2) may be defined by

$$\xi = \left\{ \frac{x^2 - x_\ell^2(\eta)}{x_t^2(\eta) - x_\ell^2(\eta)} \right\} \quad , \qquad (12)$$

lines of constant ξ being given by

$$x = \left[\xi\, x_t^2(\eta) + (1-\xi)\, x_\ell^2(\eta) \right]^{\frac{1}{2}} \quad . \qquad (13)$$

Using the definitions (9) and (11), these lines are seen to be smooth and regular as required by (B), except of course the line corresponding to $\xi = 0$ which describes the cranked leading edge. Coordinate lines from (13) are illustrated in Figure 6b.

Using the coordinates ξ,η (henceforth ξ will be defined by (12)) the required singular variations of the loading representation are simply constructed. Referring to (8), the conical apex singularity form is applicable to straight leading edges; however it may be applied to a more general leading edge shape by rewriting the variable u as follows.

From (7) $\quad u = \left(\frac{\cos\theta-\cos y}{1-\cos\theta\cos y}\right)$,

and writing $\cos\theta = \frac{x}{\sqrt{x^2+y^2}}$, $\cos y = \frac{x_\ell}{\sqrt{x_\ell^2+y^2}}$,

there results, after manipulation,

$$u = \left(\frac{x^2-x_\ell^2}{rx + x_\ell\sqrt{x_\ell^2+y^2}}\right) ,$$

which reduces to the original form if x_ℓ is linear. The required trailing edge singularity, i.e. $\{x_t-x\}^{\frac{1}{2}}$, may be written without loss of generality as $\{x_t^2-x^2\}^{\frac{1}{2}}$ and that at the tip as $\{1-\eta^2\}^{\frac{1}{2}}$. Thus, using the 'inner' solution form in (8), the singular content of a fully matched loading representation may be written as

$$r^{\nu_o-1}\cdot\left\{\frac{rx + x_\ell\sqrt{x_\ell^2+y^2}}{x^2-x_\ell^2}\right\}^{\frac{1}{2}}\cdot\{x_t^2-x^2\}^{\frac{1}{2}}\{1-\eta^2\}^{\frac{1}{2}} .$$

Using this expression, and noting that

$$\left(\frac{x_t^2-x^2}{x^2-x_\ell^2}\right) = \left(\frac{1-\xi}{\xi}\right) ,$$

a fully matched loading representation takes the general form

$$\Delta C_p = r^{\nu_o - 1} \{rx + x_\ell \sqrt{x_\ell^2 + y^2}\}^{\frac{1}{2}} \sqrt{\frac{1-\xi}{\xi}} \sqrt{1-\eta^2} \cdot \Delta C_p^*$$

where $\Delta C_p^* (\xi, \eta)$ is a regular function of ξ and η.

The simplest logical approximation to ΔC_p^* may be written as

$$\Delta C_p^* = \sum_{i=o}^{n-1} \sum_{j=0}^{m-1} a_{ij} \xi^i \eta^{2j} \quad .$$

However, since the coordinates ξ, η no longer take account of the conical form of the regular part of the 'inner' solution, i.e. of $F_o(u,y)$, it was decided to assess the near apex capabilities of this simple ΔC_p^* form before attempting to implement its use in the double integral. The resulting fitting exercise showed conclusively that only forms for ΔC_p^* which explicitly include the function F_o could be regarded as suitable. Two such possible forms are

$$\Delta C_p^* = aF_o(u,y) + \sum_{i=0}^{(n-1)} \sum_{j=0}^{(m-1)} b_{ij} \xi^i \eta^{2j} \quad , \qquad (14a)$$

and

$$\Delta C_p^* = F_o(u,y) \sum_{i=0}^{(n-1)} \sum_{j=0}^{(m-1)} c_{ij} \xi^i \eta^{2j} \quad , \qquad (14b)$$

however, it will be shown later that the additive representation in (14a) is decidedly inferior to the multiplicative form in (14b).

4. COMMENTS ON THE TREATMENT OF CROPPED DELTA PLANFORMS REPORTED IN REFERENCE 13

In order to assess the practicality of the coordinate system and loading representation introduced in Section 3.3.2.2, it was decided to apply these to a simple class of planforms so that results could be obtained within a reasonably short timescale. The planforms chosen constitute the cropped delta class and are defined by,

$$x_\ell(\eta) = \alpha |\eta|$$

$$x_t(\eta) = c_R \quad , \qquad \text{(a constant)}$$

where $c_R = \left(\frac{\alpha}{1-\lambda}\right)$, with λ the taper ratio; (with no loss of generality unit semispan is assumed).

From (12) and (13),

$$\xi = \left(\frac{x^2-\alpha^2\eta^2}{d(\eta)}\right) , \quad x = \{\alpha^2\eta^2 + d(\eta)\xi\}^{\frac{1}{2}} , \tag{15}$$

where $d(\eta) = (c_R^2 - \alpha^2\eta^2)$,

and the loading representation is,

$$\Delta C_p = r^{\nu_o - 1} \{rx + \alpha\eta^2\sqrt{1+\alpha^2}\}^{\frac{1}{2}} \sqrt{\frac{1-\xi}{\xi}} \sqrt{1-\eta^2}\, \Delta C_p^* ,$$

with $r = (x^2+\eta^2)$.

Chebyshev polynomials are introduced into the representation for ΔC_p^*, so that it is rewritten as

$$\Delta C_p^* = F_o(u,y) \sum_{i=0}^{(n-1)} \sum_{j=0}^{(\bar{m}-1)} a_{ij}\, T_i(2\xi-1)\, T_{2j}(\eta) . \tag{16a}$$

In order to investigate the effect of the function $F_o(u,y)$, a representation was also considered in which the function was omitted, i.e.

$$\Delta C_p^* = \sum_{i=0}^{(n-1)} \sum_{j=0}^{(\bar{m}-1)} a_{ij}\, T_i(2\xi-1)\, T_{2j}(\eta) \tag{16b}$$

The alternative representations in (16a) and (16b) are referred to as 'including F' and 'excluding F', respectively.

Introducing (15) into (1) and noting that

$$dx\, dy = dx\, d\eta = \frac{d(\eta) d\xi\, d\eta}{2x} ,$$

the basic incompressible equation becomes,

$$\frac{W}{U}(\xi_r,\eta_s) = -\frac{1}{16\pi} \int_0^1 \int_{-1}^1 \frac{\Delta C_p\, d(\eta)}{x} \left\{1 - \frac{X}{R}\right\} \frac{d\eta\, d\xi}{(\eta-\eta_s)^2} ,$$

with $X = (x-x_r)$, $R = \{(x-x_r)^2 + (\eta-\eta_s)^2\}$ and
ξ as defined in (15).

Introducing the loading representation, $\frac{W}{U}$ is defined in terms of downwash modes through

$$\frac{W}{U}(\xi_r,\eta_s) = -\frac{1}{16\pi}\sum_{i=0}^{(n-1)}\sum_{j=0}^{(\bar{m}-1)} a_{ij}\, W_{ij}(\xi_r,\eta_s) \quad , \tag{17}$$

where the downwash modes are defined by,

$$W_{ij}(\xi_r,\eta_s) = \int_0^1 T_i(2\xi-1)\sqrt{\frac{1-\xi}{\xi}}\int_{-1}^{1} T_{2j}(\eta)K(\xi,\eta)\sqrt{1-\eta^2}\left\{1-\frac{X}{R}\right\}\frac{d\eta\, d\xi}{(\eta-\eta_s)^2} \quad , \tag{18}$$

with

$$K(\xi,\eta) = \frac{r^{\nu_o-1}\{rx + \alpha\eta^2\sqrt{1+\alpha^2}\}^{\frac{1}{2}}\, d(\eta)\;\; F_o(u,\gamma)}{x} \quad . \tag{19}$$

For the ΔC_p^* representation in (16b), $F_o(u,\gamma)$ is omitted from (19).

4.1 Evaluation of the Downwash Modes

The expression (18) for the downwash modes is analogous to the corresponding expression (5) for regular planforms, so that the techniques developed for the latter (Reference 2) can be extended to apply to the present case. Particular complications arise in the present case mainly due to the presence of the term $K(\xi,\eta)$ in the spanwise integration.

$K(\xi,\eta)$ is infinite at the apex ($\xi = \eta = 0$), and in the neighbourhood of the centreline ($\eta = 0$) exhibits rapid variations for ξ small; as illustrated in Figure 7. Also, because of the presence of $K(\xi,\eta)$ it is in general impossible to perform an analytic evaluation of the finite part integral.

A computer program has been written in IBM System/360 Fortran IV to evaluate the downwash modes from (18), using developments of the techniques of Reference 2. In order to obtain results within a short timescale, the program was not written to cover all parametric cases. In particular, for η_s either at the centreline or in its immediate neighbourhood it was found that special integration techniques are required in order to maintain the accuracy of spanwise integrations and these could not be incorporated within the timescale. In the chordwise integration a similar problem was found for ξ_r approaching the leading edge.

Thus the program that evaluates the downwash modes is restricted in that ξ_r and/or η_s cannot be positioned arbitrarily close to zero. However, this did not prevent collocation solutions from being obtained since one is not forced to choose collocation points in these positions. In practice, the downwash modes have been evaluated for ξ_r, η_s = 0.01, with no apparent loss of accuracy.

4.2 Numerical Results

Numerical results have been obtained for a particular flatplate cropped delta planform with 45° leading edge sweep and taper ratio 1/7, (Aspect Ratio 3), at unit incidence (W/U = 1).

For this leading edge sweep, the value of ν_o was taken from Rossiter[11] as,

$$\nu_o = 0.8145 \quad \text{(see also Section 3.2.1)}$$

For the function $F_o(u,\gamma)$, the expansion due to Taylor[12] was used. This function, which is plotted in Figure 5 against the variable η/x, is simply approximated in terms of the variable u by the quadratic,

$$F(u) = \frac{F_o(u,\frac{\pi}{4})}{F_o(1,\frac{\pi}{4})} = (0.7646 + 0.2555u - 0.0201u^2) \quad .$$

4.2.1 Collocation Distributions for Loading Solutions

Loading solutions are obtained by solving the relation (17) for the $\bar{m}n$ unknowns a_{ij} by specifying the downwash $\frac{W}{U}(\xi_r,\eta_s)$ at $\bar{m}n$ collocation points (ξ_r,η_s). For a loading representation that contains the form (14a), the relation (17) will be slightly modified, however this will be considered later.

The collocation distributions chosen were of the standard Multhopp type in the new coordinates. In the spanwise sense only even distributions were used, so that there is not a collocation station at η_s = 0. In the chordwise sense, since the loading is defined in terms of polynomials in ξ, the collocation distribution is chosen as a Multhopp distribution in ξ_r.

Thus the spanwise distribution is,

$$\eta_s = \cos\left(\frac{s\pi}{2\bar{m}+1}\right) \quad , \quad s = 1, \bar{m} \quad .$$

For the chordwise distribution, if

$$\zeta_r = \frac{1}{2}\left\{1 - \cos\left(\frac{2r\pi}{2n+1}\right)\right\} , \quad r = 1, n ,$$

then the distribution is,

$$\xi_r = \zeta_r , \qquad r = 1, n .$$

A usual chordwise distribution, as used for regular planforms, would be in terms of a percentage chord variable, i.e. if,

$$\bar{x} = \frac{x - x_\ell(\eta)}{c(\eta)} , \tag{20}$$

then the normal distribution would be,

$$\bar{x}_r = \zeta_r , \qquad r = 1, n .$$

Thus the collocation distribution used is, from (15),

$$x_{rs} = \{a^2\eta_s^2 + d(\eta_s)\,\zeta_r\}^{\frac{1}{2}} ,$$

whereas the usual distribution, as applied to the cropped delta, would be,

$$x_{rs} = \{a|\eta_s| + c(\eta_s)\zeta_r\} .$$

The two distributions are compared in Figure 8 for $(2\bar{m},n) = (14,5)$.

In what follows the order of a loading solution is written in terms of the number of collocation stations on the full span, i.e. $2\bar{m} = m$ spanwise, and n chordwise. Thus the order of solution is denoted by (m,n).

For comparison purposes, some solutions have also been obtained using the regular planform programs. For these solutions, the planform is rounded inboard of $|\eta| = 0.2$, and the chordwise collocation distribution is of the usual type, i.e. $\bar{x}_r = \zeta_r$ as above.

4.2.2 Loading Solutions

Table 1 compares the ΔC_p distributions obtained from the cranked planform program solutions, both 'including F' and 'excluding F', and the regular planform program solution. The solutions are for (m,n) = (16,5) and results are given along six spanwise stations at chordwise stations $\bar{x}$ defined by (20). At $\eta = 0$, the regular planform values cannot be strictly compared since the $\bar{x}$ stations correspond to different points in space due to the planform rounding, however the values are included for completeness. For $\eta \geq 0.2$, a strict comparison is valid.

Away from $\eta = 0$, the cranked planform solutions and regular planform solutions are in quite good agreement. In particular, the cranked planform solution 'including F' is closer to the regular planform solution than the cranked planform solution 'excluding F'. It should be noted that (m,n) = (16,5) does not represent a converged solution for any of the three loading forms, so that exact agreement is not expected.

At $\eta = 0$, the two cranked planform solutions are considerably different. Figure 9 compares the convergence with increasing m of the two cranked planform solutions at $\eta = 0$. The two (24,5) solutions are compared in Figure 10. Figure 9 indicates that by including the special function in the loading representation, the convergence of the solution is greatly improved. Accepting the (24,5) solution 'including F' to be close to convergence, then the solution 'excluding F' is clearly unsatisfactory. It can be inferred that a prohibitive number of terms would be required to achieve convergence for this latter solution. This inference can also be made by considering the variation of the downwash modes.

Figures 11 and 12 illustrate the η_s variation of the first few spanwise downwash modes along the constant ξ_r line, $\xi_r = 0.0794$, which corresponds to the first chordwise collocation station for n = 5. From (17) the required downwash is to be represented by a linear combination of downwash modes. Referring to Figure 11, for the loading representation 'excluding F', the rapid variation of the modes near $\eta_s = 0$ indicate that these modes are unsuitable for the representation of smooth downwash variations. In obtaining collocation solutions, as the number of spanwise loading terms is increased the most inboard η_s collocation station is positioned closer to the centreline and hence the effect of the local rapid variations is more apparent.

Referring to Figure 12, the benefit of including the special function in the loading representation is well illustrated. The downwash modes for the representation 'including F' vary smoothly in the centreline region and hence are well suited for the representation of smooth downwash variations. It is to be noted that both loading representations result in rapid variations in the downwash modes in the tip region, i.e. η_s near 1, thus illustrating the inadequacy of the assumed loading representations near the leading edge tip corner.

Consideration of the downwash modes also indicates the unsuitability of the loading form in (14a), since that representation would require the downwash to be represented by a combination of the W_{oo} mode of Figure 12 and the unsatisfactory modes of Figure 11.

The convergence with increasing chordwise terms of 'including F' solutions is illustrated in Table 2, where ΔC_p distributions at six spanwise stations are presented for $(m,n) = (14,4)$, $(14,5)$, $(14,8)$, $(14,9)$. The distributions at $\eta = 0$ are also plotted in Figure 13.

4.2.3 Downwash Interpolation

The previous section describes various loading solutions obtained through satisfying (17) at $\bar{m}n$ collocation stations on the half planform. Substituting the loading solutions back into (17), the downwash can be evaluated at any point on the planform. (With the present program this excepts the region ξ_r, $\eta_s < \epsilon$, with $\epsilon = 0.01$, approximately.) Evaluation of the downwash at points other than the collocation points used to obtain the loading solution, is here referred to as downwash interpolation. Ideally, for the planform considered, the downwash should be unity at all points on the planform, so that the discrepancy of the interpolated downwash from unity is a measure of the accuracy of a loading solution.

In the previous section, the advantage of including the special function in the loading representation was demonstrated. This is further illustrated in this section by comparing downwash interpolations.

Figure 14 compares the chordwise downwash interpolation at the first spanwise collocation station, $\eta_s = 0.1045$, of the $(14,5)$ solutions. On the evidence of this figure there is little to choose between the two solutions. Over most of the range the discrepancies from unity are less than 1%, but larger discrepancies are inferred at the leading edge.

The remainder of the downwash interpolations are for the $(16,5)$ solutions. The various interpolation lines are shown in Figure 15.

Figure 16 compares the spanwise downwash interpolation at the first chordwise collocation station, $\xi_r = 0.0794$. The advantage of including the special function is clearly illustrated by the improved variation in the centreline region. Also included in Figure 16 is the corresponding downwash interpolation from the regular planform solution, for comparison. The rapid variation in the neighbourhood of $\eta_s = 1$ is an indication of the effect of the inadequacy of the loading representation in the leading edge tip corner region, as mentioned in the previous section.

Figure 17 compares the spanwise downwash interpolation at a chordwise collocation station nearer the trailing edge, $\xi_r = 0.5712$. Surprisingly perhaps, the solution 'excluding F' again shows a large discrepancy near $\eta_s = 0$.

Figure 18 compares the chordwise downwash interpolation at the station $\eta_s = 0.01$ and it is seen that the solution 'excluding F' shows a large discrepancy over most of the range.

Finally, Figure 19 compares the spanwise downwash interpolation at a station close to the leading edge i.e. $\xi_r = 0.01$. Again, the advantage of 'including F' is apparent in the centreline region but the effect of the tip corner loading deficiency is now more obvious.

5. CONCLUDING REMARKS

An account has been given of a line of research which reveals a gradual development of ideas that, in general, connect the successful treatments of 'regular' and 'irregular' planforms. The 'irregular' planforms considered were restricted to the cropped delta type, but the principles which guided the derivation and assessment of the method are of general value. The most important of these principles may be summarised by the following statements.

(i) Determine the analytic form of special loading variations required by the imposed boundary conditions (see (A) of Section 2.1).

(ii) Choose coordinates suitable for integration (see (B) and (C) of Section 2.1).

(iii) Using (i) and (ii) select a modal form for the fully matched loading which yields a set of downwash modes which are compatible in the sense of Section 3.3.

Using (i), the concept of matched asymptotic expansions led to recognising the practical usefulness of the infinite sector solutions, and this was verified through the work described in Section 3.2.1. Implications of (ii) eventually led to the choice of integration coordinates made in Section 3.3.2.2 and (iii) helped in judging the relative merits of the fully matched loading representations used in Section 4.

Using the experience gained during the currently reviewed work program, it is foreseen that convergent treatments are possible for symmetric planforms having both their leading and trailing edges cranked at the centre section. Also, an improvement of solution quality in the tip regions is envisaged.

Symbols

a_{ij} Coefficients used in defining loading representations

C_p Pressure coefficient

c Local chord

c_R Root chord value *i.e.* $c_R = c(0)$

d Function defined in equation (15)

F_o Function used in equation (8) to define the infinite sector form for ΔC_p

f_i Eigenfunctions associated with the infinite sector problem

K Function defined in equation (19)

M Free stream Mach number

m In Section 4 onwards refers to the total number (even) of spanwise collocation stations

$\bar{m}$ The number of spanwise collocation stations on the half span *i.e.* $\bar{m} = \frac{m}{2}$

n The number of chordwise collocation points along each spanwise collocation station

R As defined in equation (5)

r Radial distance from local apex origin. Also, subscript designating a collocation point coordinate.

s Semi span of the planform. Also, subscript designating a collocation point coordinate.

T_n Chebyshev polynomial of order n

U Free stream speed

u Variable as defined in equation (7)

W Vertical perturbation velocity

Symbols Contd.

W_{ij}	Downwash modes
X	As defined in equation (5)
x,y,z	Right handed set of cartesian coordinates
x_ℓ	x-coordinate of the planform's leading edge (see e.g. equation (9))
x_t	x-coordinate of the planform's trailing edge (see e.g. equation (11))
α	Incidence angle of the free stream
β =	$\sqrt{1-M^2}$
γ	Half angle of infinite sector or a planform edge crank
Δ	Operator giving difference between upper and lower surface planform values (see e.g. ΔC_p)
ζ	Non-dimensional coordinate defined in Section 3.3.2.1
η =	$\frac{y}{s}$ As defined in equation (2)
η_ℓ	η-coordinate of the planform's leading edge (see e.g. equation (10))
θ	Angle measured from bisector of an infinite sector or a planform edge crank
ν_i	Eigenvalues associated with the infinite sector problem
ξ	Non-dimensional coordinates defined by equation (2) for regular planforms, and by equation (12) for planforms with a leading edge crank
ϕ	Perturbation velocity potential
$_i\phi$	Eigensolutions associated with the infinite sector problem
χ	Non-dimensional coordinate defined in Section 3.3.2.1

References

No.	Author(s)	Title, etc.
1.	Hewitt, B. L.	Developments in Subsonic Lifting Surface Theory. B.A.C. (Warton) Report Ae 282, Sept. 1967, or S and T. Memo 1/69.
2.	Hewitt, B. L. Kellaway, W.	A New Treatment of the Subsonic Lifting Surface Problem Using Curvilinear Coordinates. Part I: Details of the method as applied to regular surfaces with finite tip chords and a preliminary set of numerical results. B.A.C. (Warton) Report Ae 290, August 1968, or S and T. Memo 2/69.
3.	Leclerc, J.	A New Integration Technique for the Determination of the Unsteady Aerodynamic Forces at Subsonic Speeds. La Recherche Aérospatiale, No. 112, May/June 1966, pp. 43-61.
4.	Marchbank, W. R. Kennelly, J. M. Hewitt, B. L.	The Evaluation of Pressure Distributions on Wings with Control Surfaces in Subsonic Flow. B.A.C. (Warton) Report Ae 311, November 1970.
5.	Hewitt, B. L.	Comments on a Numerical Treatment of the Subsonic Lifting Surface Theory Problem for Wings with a Centre-Section Crank. B.A.C. (Warton) Tech. Note Ae/A/315, May 1968.
6.	Germain, P.	On the Subsonic Flow in the Neighbourhood of the Apex of a Delta Wing. La Recherche Aéronautique, No. 44, March/April 1955.
7.	Legendre, R.	Subsonic Cross Flow at a Plane Angular Sector. Comptes Rendus, Tome 243, No. 22, November 1956, pp. 1716 - 1718.
8.	Hewitt, B. L.	A Reassessment of the Numerical Treatment of the Lifting Surface Theory Problem for Wings with Centre-Section Cranks in Subsonic Flow. B.A.C. (Warton) Tech. Note Ae/A/306, September 1968
9.	Hewitt, B. L. Kellaway, W.	A New Treatment of the Subsonic Lifting Surface Problem Using Curvilinear Coordinates. Part II: Numerical convergence tests and comments related to possible future development. B.A.C. (Warton) Report Ae 290, March 1969.

No.	Author(s)	Title, etc.
10.	Brown, S. N. Stewartson, K.	Flow Near the Apex of a Plane Delta Wing. J. Inst. Maths. Applics., 5, 206, 1969.
11.	Rossiter, Patricia, J.	The Centre-Section of a Lifting Swept Wing in Linearised Subsonic Flow. ARC R&M 3630. 1969.
12.	Taylor, R.	Unpublished work at University of Surrey.
13.	Kellaway, W.	Comments on the Solution of the Subsonic Lifting Surface Theory Problem for Planforms with a Centre-Section Crank. B.A.C. (Warton) Tech. Note Ae/A/327.

Table 1

Comparison of ΔC_p Distributions from Solutions with (m,n) = (16,5) for Cropped Delta Planform

ΔC_p at η = 0.0

$\bar{x}$	'Excluding F'	'Including F'	'Regular Planform'
.005	5.7897	7.4719	15.7290
.025	4.2941	5.5355	7.3498
.05	3.7725	4.8463	5.4464
.1	3.3047	4.1878	4.1387
.2	2.8541	3.4424	3.1737
.3	2.5472	2.8781	2.6518
.4	2.2543	2.3998	2.2532
.5	1.9425	1.9997	1.9081
.6	1.6147	1.6625	1.5910
.7	1.2909	1.3521	1.2870
.8	0.9819	1.0272	0.9812
.9	0.6537	0.6647	0.6460
.95	0.4429	0.4543	0.4398

ΔC_p at η = 0.2

$\bar{x}$	'Excluding F'	'Including F'	'Regular Planform'
.005	20.6434	21.0094	20.6006
.025	9.2275	9.5095	9.3351
.05	6.5271	6.8102	6.6940
.1	4.6264	4.8997	4.8319
.2	3.2797	3.4794	3.4697
.3	2.6453	2.7630	2.7933
.4	2.2104	2.2768	2.3220
.5	1.8531	1.9040	1.9401
.6	1.5327	1.5869	1.6038
.7	1.2326	1.2846	1.2901
.8	0.9386	0.9711	0.9806
.9	0.6203	0.6330	0.6458
.95	0.4229	0.4357	0.4405

Table 1 (Continued) Comparison of ΔC_p Distributions from Solutions with (m,n) = (16,5) for Cropped Delta Planform

ΔC_p at η = 0.4

$\bar{x}$	'Excluding F'	'Including F'	'Regular Planform'
.005	26.4373	27.1839	27.3460
.025	11.7634	12.1091	12.1569
.05	8.2622	8.5135	8.5283
.1	5.7549	5.9353	5.9252
.2	3.9164	4.0348	4.0132
.3	3.0347	3.1189	3.1008
.4	2.4511	2.5153	2.5035
.5	2.0024	2.0553	2.0485
.6	1.6271	1.6722	1.6681
.7	1.2941	1.3305	1.3275
.8	0.9783	1.0040	1.0016
.9	0.6425	0.6582	0.6567
.95	0.4368	0.4485	0.4475

ΔC_p at η = 0.6

$\bar{x}$	'Excluding F'	'Including F'	'Regular Planform'
.005	32.4925	33.1170	33.0318
.025	14.3910	14.6700	14.6369
.05	10.0496	10.2461	10.2273
.1	6.9210	7.0577	7.0507
.2	4.6117	4.7033	4.7048
.3	3.5099	3.5797	3.5820
.4	2.7936	2.8496	2.8497
.5	2.2541	2.3000	2.2975
.6	1.8098	1.8472	1.8440
.7	1.4202	1.4498	1.4478
.8	1.0582	1.0801	1.0802
.9	0.6883	0.7026	0.7032
.95	0.4688	0.4788	0.4785

Table 1 (Continued) Comparison of ΔC_p Distributions from Solutions with (m,n) = (16,5) for Cropped Delta Planform

ΔC_p at η = 0.8

$\bar{x}$	'Excluding F'	'Including F'	'Regular Planform'
.005	39.6307	40.2038	39.9057
.025	17.4545	17.7074	17.5980
.05	12.1074	12.2831	12.2269
.1	8.2342	8.3538	8.3421
.2	5.3648	5.4429	5.4623
.3	3.9989	4.0579	4.0802
.4	3.1157	3.1627	3.1768
.5	2.4554	2.4936	2.4980
.6	1.9198	1.9505	1.9493
.7	1.4642	1.4880	1.4868
.8	1.0627	1.0801	1.0818
.9	0.6814	0.6927	0.6949
.95	0.4650	0.4730	0.4734

ΔC_p at η = 0.9

$\bar{x}$	'Excluding F'	'Including F'	'Regular Planform'
.005	42.0171	42.5743	42.8826
.025	18.6593	18.9047	19.0143
.05	13.0348	13.2054	13.2562
.1	8.9031	9.0199	9.0182
.2	5.6655	5.7419	5.7033
.3	4.0009	4.0563	4.0191
.4	2.9069	2.9475	2.9268
.5	2.1363	2.1659	2.1613
.6	1.5827	1.6047	1.6069
.7	1.1757	1.1928	1.1919
.8	0.8524	0.8657	0.8590
.9	0.5449	0.5535	0.5492
.95	0.3645	0.3699	0.3711

Table 2 Comparison of ΔC_p Distributions from 'Including F' Solutions with (m,n) = (14,4), (14,5), (14,8), (14,9) for Cropped Delta Planform

ΔC_p at $\eta = 0.0$

$\bar{x}$	(14,4)	(14,5)	(14,8)	(14,9)
.005	7.4409	7.5722	7.7835	7.8198
.025	5.5136	5.6091	5.7603	5.7855
.05	4.8298	4.9087	5.0267	5.0446
.1	4.1827	4.2349	4.2917	4.2949
.2	3.4631	3.4609	3.4094	3.3949
.3	2.9151	2.8718	2.7978	2.7948
.4	2.4307	2.3805	2.3636	2.3714
.5	2.0045	1.9823	2.0099	2.0080
.6	1.6411	1.6564	1.6685	1.6651
.7	1.3298	1.3556	1.3432	1.3475
.8	1.0331	1.0301	1.0252	1.0219
.9	0.6830	0.6627	0.6690	0.6722
.95	0.4526	0.4543	0.4583	0.4564

ΔC_p at $\eta = 0.2$

$\bar{x}$	(14,4)	(14,5)	(14,8)	(14,9)
.005	20.5974	20.7744	21.0038	21.0382
.025	9.3504	9.4160	9.4831	9.4889
.05	6.7221	6.7555	6.7726	6.7697
.1	4.8750	4.8790	4.8548	4.8472
.2	3.5133	3.4910	3.4552	3.4540
.3	2.8142	2.7873	2.7770	2.7808
.4	2.3158	2.2995	2.3103	2.3104
.5	1.9158	1.9163	1.9258	1.9234
.6	1.5764	1.5879	1.5860	1.5872
.7	1.2724	1.2808	1.2759	1.2767
.8	0.9753	0.9705	0.9700	0.9686
.9	0.6426	0.6353	0.6378	0.6391
.95	0.4335	0.4354	0.4366	0.4354

Table 2 (Continued)

Comparison of ΔC_p Distributions from 'Including F' Solutions with (m,n) = (14,4), (14,5), (14,8), (14,9) for Cropped Delta Planform

ΔC_p at $\eta = 0.4$

$\bar{x}$	(14,4)	(14,5)	(14,8)	(14,9)
.005	27.4074	27.5175	27.5455	27.5403
.025	12.1965	12.2282	12.2359	12.2370
.05	8.5641	8.5724	8.5742	8.5767
.1	5.9552	5.9450	5.9428	5.9448
.2	4.0277	4.0101	4.0085	4.0083
.3	3.1001	3.0902	3.0928	3.0926
.4	2.4941	2.4961	2.5010	2.5015
.5	2.0390	2.0492	2.0519	2.0521
.6	1.6655	1.6753	1.6734	1.6731
.7	1.3338	1.3349	1.3316	1.3318
.8	1.0120	1.0040	1.0047	1.0048
.9	0.6607	0.6567	0.6590	0.6588
.95	0.4455	0.4496	0.4492	0.4494

ΔC_p at $\eta = 0.6$

$\bar{x}$	(14,4)	(14,5)	(14,8)	(14,9)
.005	32.8129	32.7851	32.8101	32.8161
.025	14.5662	14.5630	14.5665	14.5658
.05	10.1986	10.2030	10.2016	10.2000
.1	7.0548	7.0640	7.0621	7.0618
.2	4.7284	4.7354	4.7369	4.7379
.3	3.6064	3.6074	3.6085	3.6084
.4	2.8680	2.8641	2.8635	2.8632
.5	2.3076	2.3025	2.3022	2.3026
.6	1.8464	1.8439	1.8453	1.8456
.7	1.4452	1.4472	1.4487	1.4484
.8	1.0768	1.0813	1.0806	1.0807
.9	0.7032	0.7039	0.7032	0.7033
.95	0.4807	0.4777	0.4783	0.4781

Table 2 (Continued)

Comparison of ΔC_p Distributions from 'Including F' Solutions with (m,n) = (14,4), (14,5), (14,8), (14,9) for Cropped Delta Planform

ΔC_p at $\eta = 0.8$

$\bar{x}$	(14,4)	(14,5)	(14,8)	(14,9)
.005	39.8969	39.9793	40.0416	40.0410
.025	17.6252	17.6408	17.6463	17.6432
.05	12.2653	12.2616	12.2519	12.2535
.1	8.3810	8.3657	8.3517	8.3518
.2	5.4803	5.4687	5.4678	5.4676
.3	4.0784	4.0776	4.0861	4.0868
.4	3.1657	3.1726	3.1791	3.1793
.5	2.4875	2.4958	2.4946	2.4943
.6	1.9450	1.9491	1.9436	1.9437
.7	1.4889	1.4868	1.4845	1.4849
.8	1.0856	1.0804	1.0840	1.0838
.9	0.6940	0.6929	0.6951	0.6952
.95	0.4693	0.4723	0.4707	0.4709

ΔC_p at $\eta = 0.9$

$\bar{x}$	(14,4)	(14,5)	(14,8)	(14,9)
.005	43.0869	42.7830	42.8137	42.8166
.025	18.9992	18.9614	18.9552	18.9542
.05	13.1801	13.2186	13.2081	13.2075
.1	8.9256	9.0024	9.0000	9.0008
.2	5.6730	5.7161	5.7221	5.7224
.3	4.0500	4.0402	4.0396	4.0390
.4	2.9809	2.9426	2.9385	2.9387
.5	2.2023	2.1680	2.1688	2.1695
.6	1.6160	1.6086	1.6146	1.6144
.7	1.1730	1.1948	1.1978	1.1974
.8	0.8366	0.8654	0.8610	0.8614
.9	0.5540	0.5534	0.5509	0.5507
.95	0.3925	0.3709	0.3738	0.3735

Produced in England by Her Majesty's Stationery Office, Reprographic Centre, Basildon

R 22044/R54 425 7/75 P

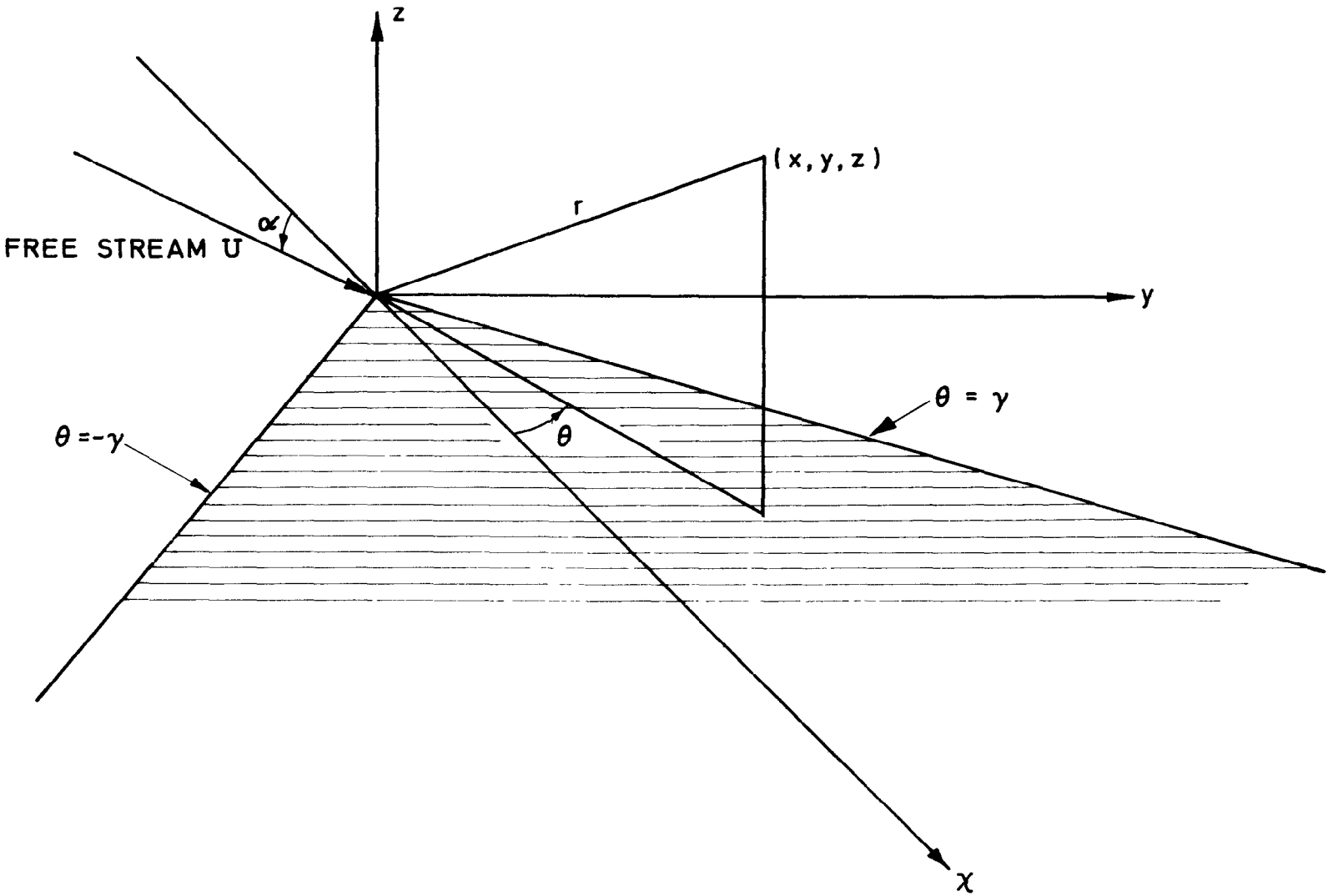

FIG.1. COORDINATE SYSTEM FOR INFINITE SECTOR

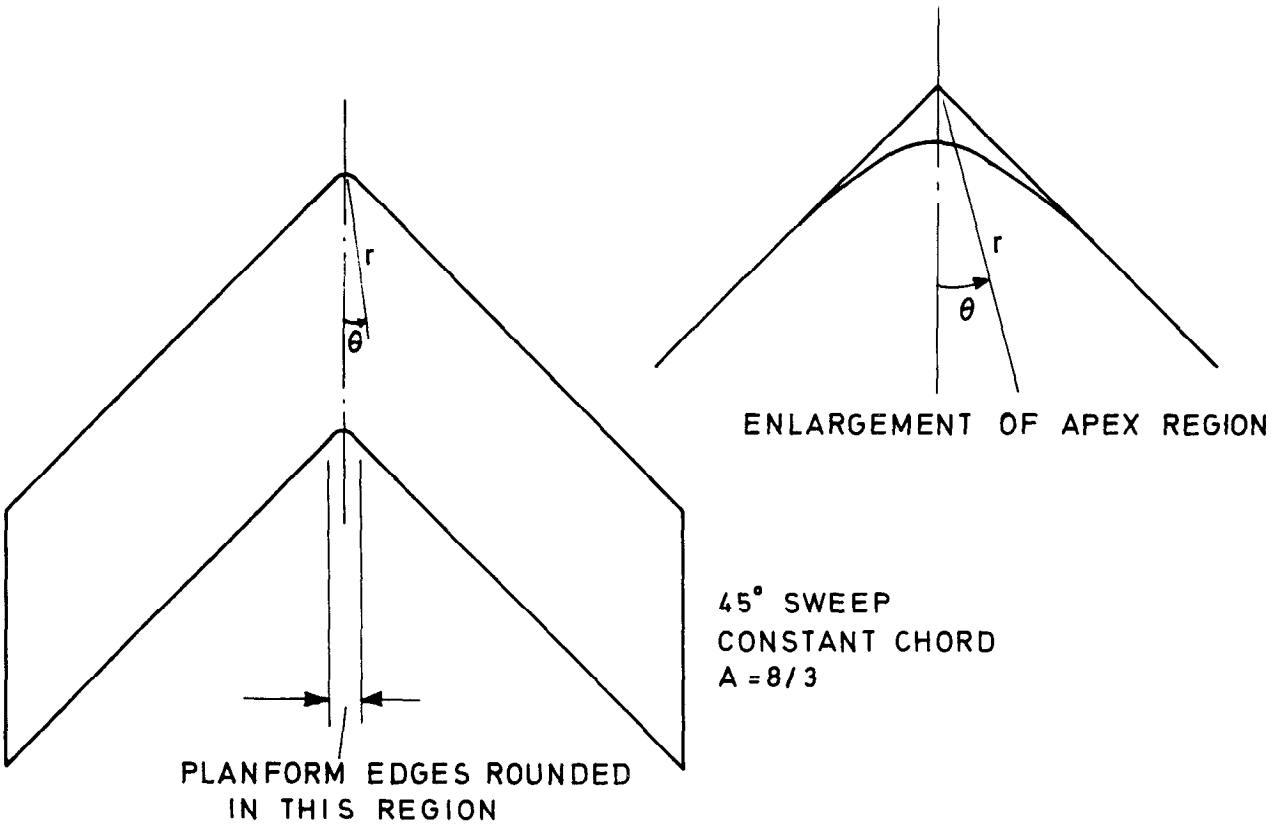

FIG. 2A. ROUNDED PLANFORM USED TO ILLUSTRATE CRANK SOLUTION BEHAVIOUR

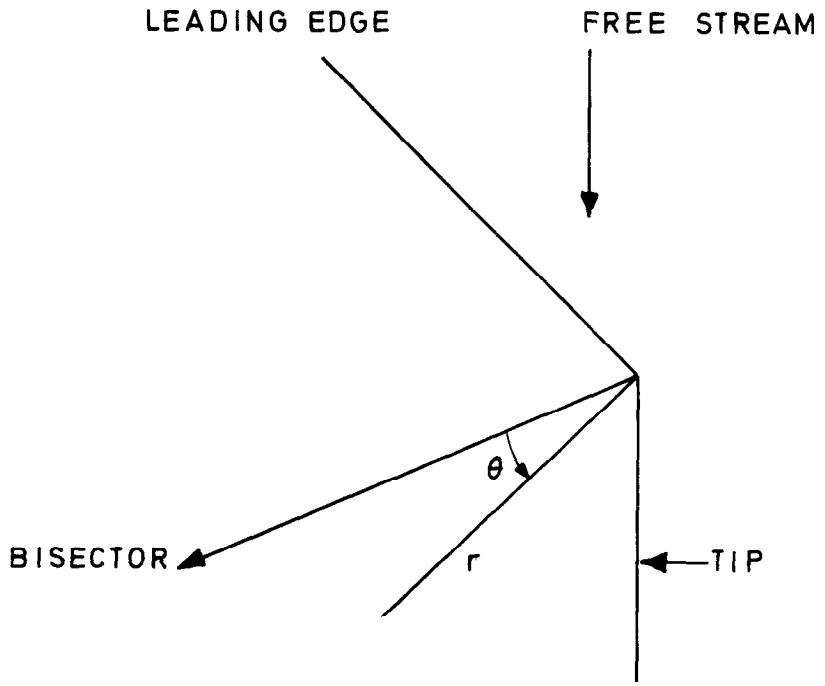

FIG. 2B. (r, θ) COORDINATES FOR LEADING EDGE-TIP INTERSECTION

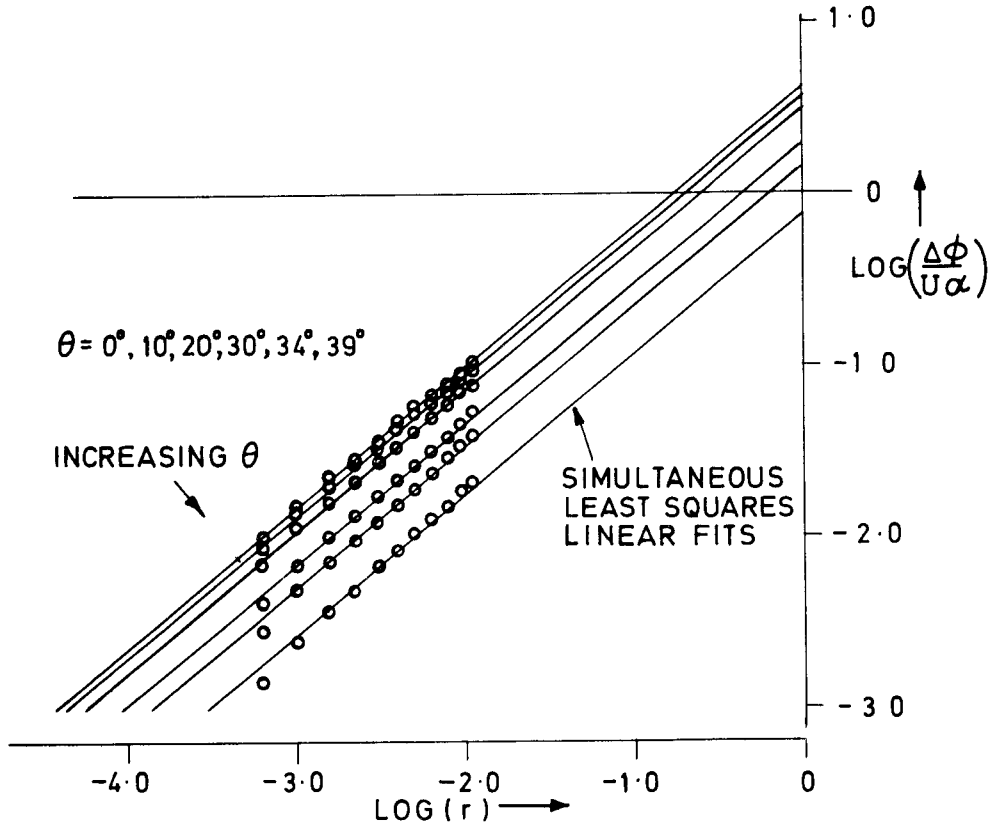

FIG. 3. VARIATION OF LOG ($\Delta\phi/U\alpha$) WITH LOG(r) ALONG LINES OF CONSTANT θ FOR PLANFORM OF FIG. 2A.

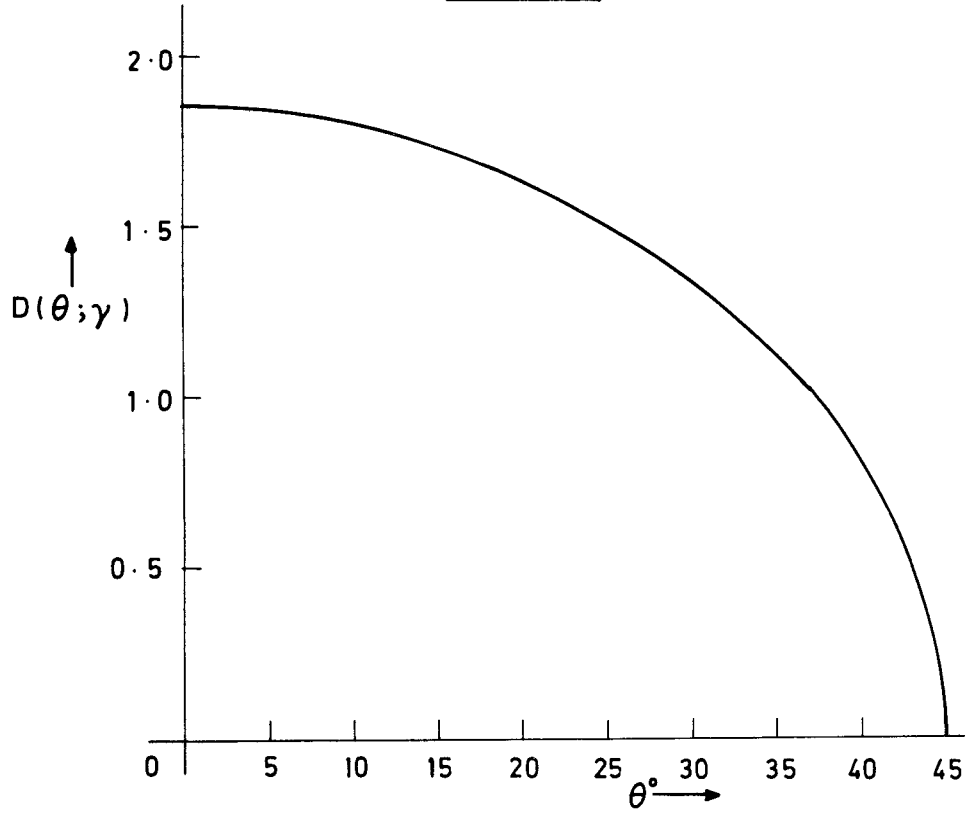

FIG. 4. THE FUNCTION $D(\theta, \gamma)$ FOR $\gamma = \pi/4$

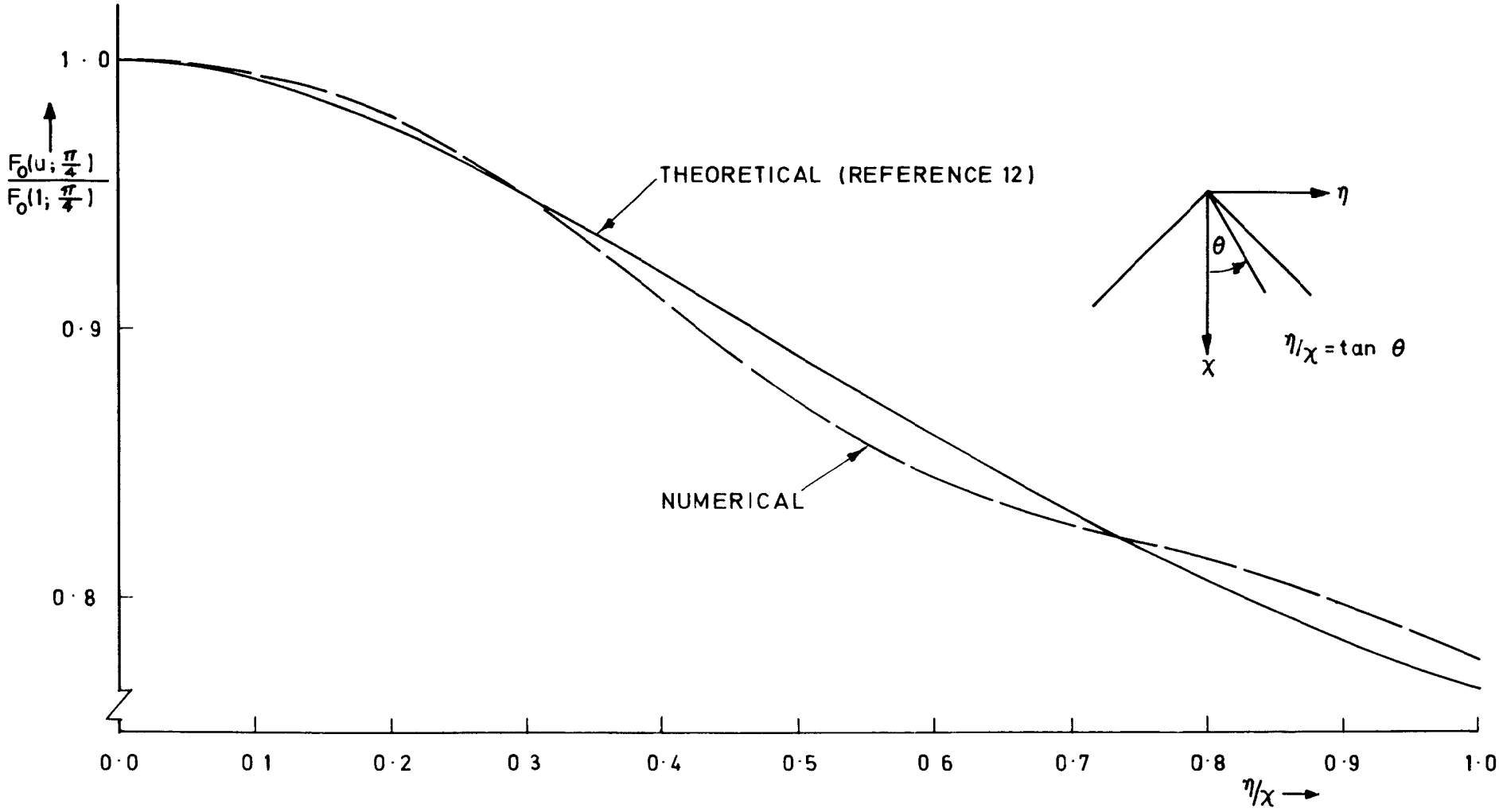

FIG.5. COMPARISON OF NUMERICAL RESULTS FOR $F_0(u;\frac{\pi}{4})$ WITH THEORETICAL EXSPANSION OF REFERENCE 12.

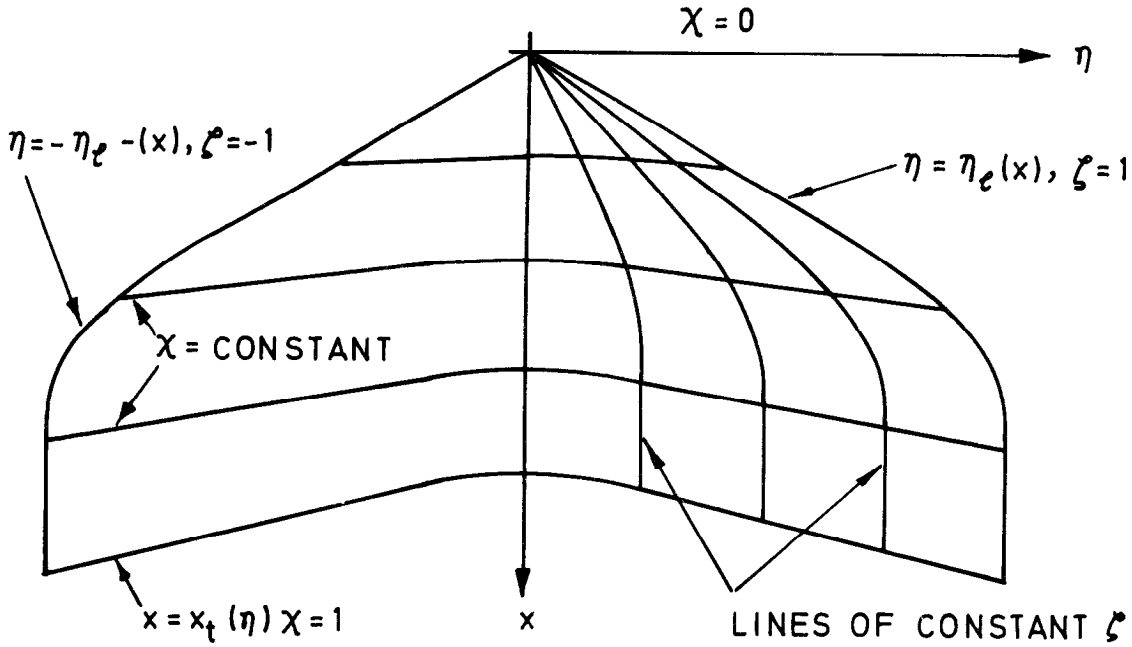

FIG. 6A. ILLUSTRATION OF ζ, χ COORDINATES.

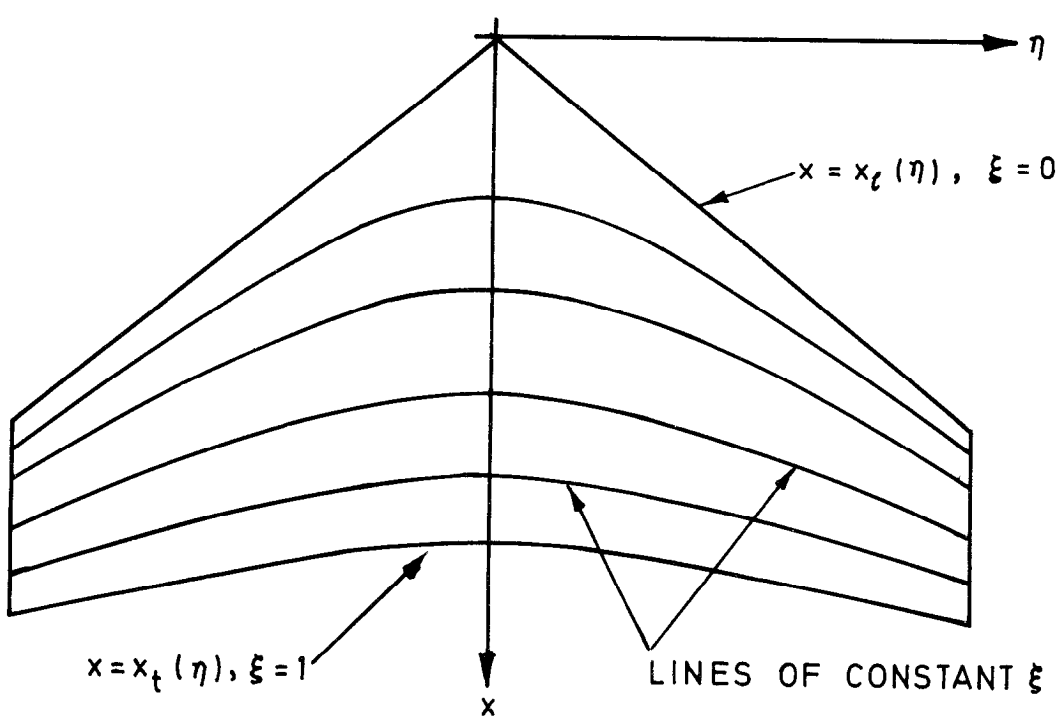

FIG. 6B. ILLUSTRATION OF ξ COORDINATE OF EQUATION 12

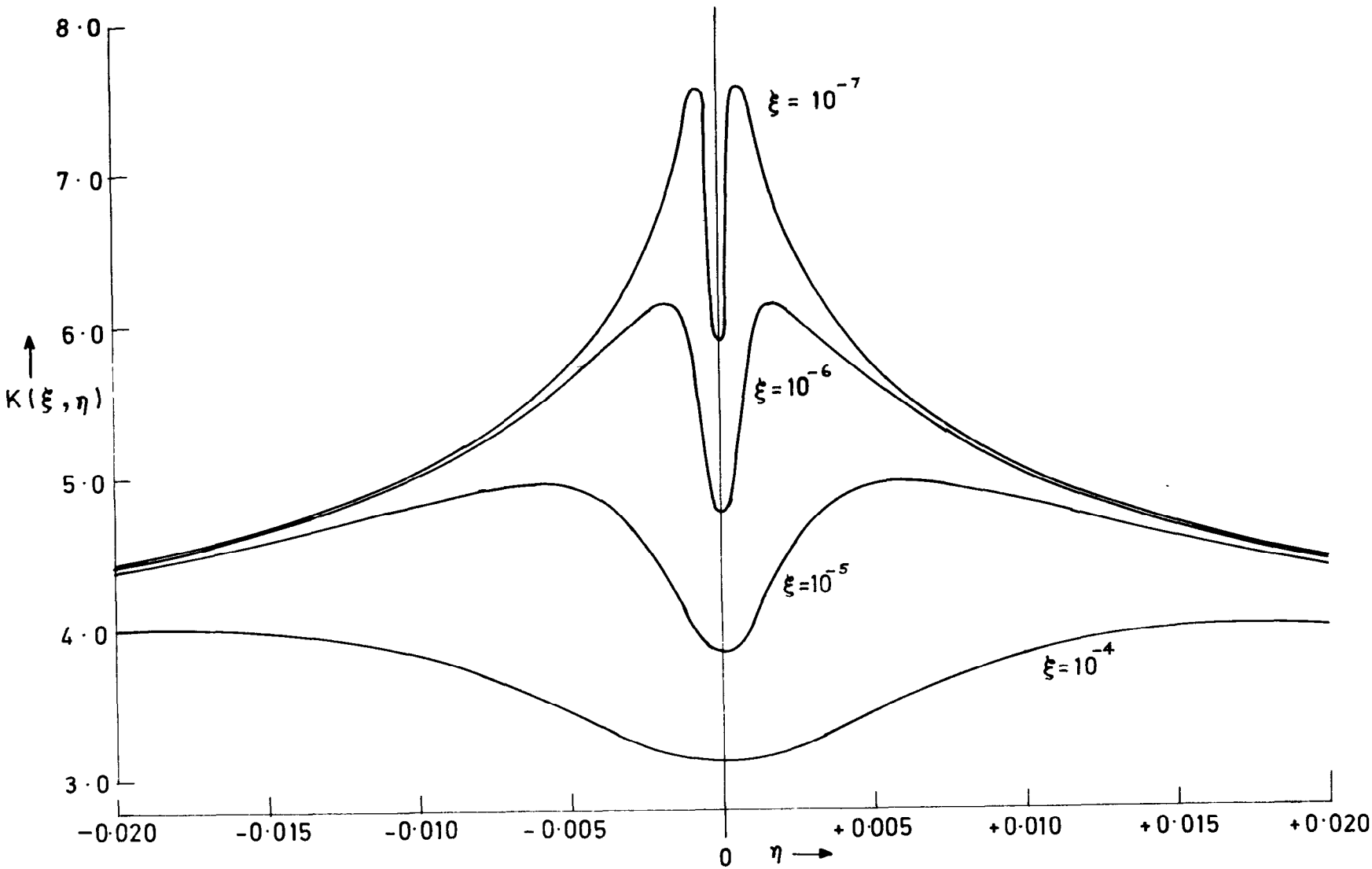

FIG.7. VARIATION OF $K(\xi,\eta)$ IN CENTRELINE REGION FOR ξ SMALL

SPANWISE DISTRIBUTION	$\eta_s = \cos\left(\frac{s\pi}{m+1}\right)$
CHORDWISE DISTRIBUTION	$\zeta_r = \frac{1}{2}\left\{1-\cos\left(\frac{2r\pi}{2n+1}\right)\right\}$

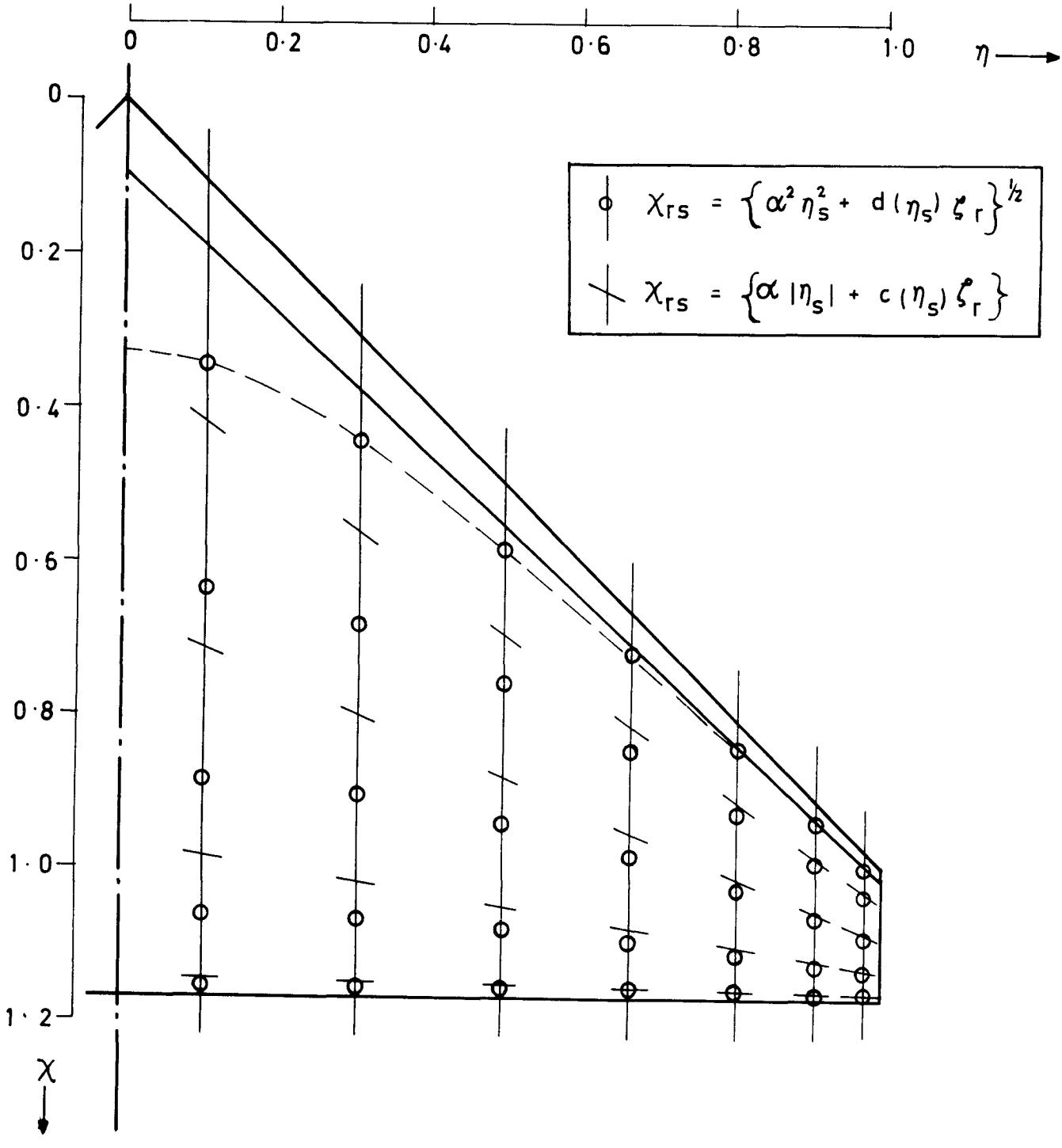

FIG.8. COMPARISON OF COLLOCATION DISTRIBUTIONS FOR CROPPED DELTA. (m,n) = (14, 5).

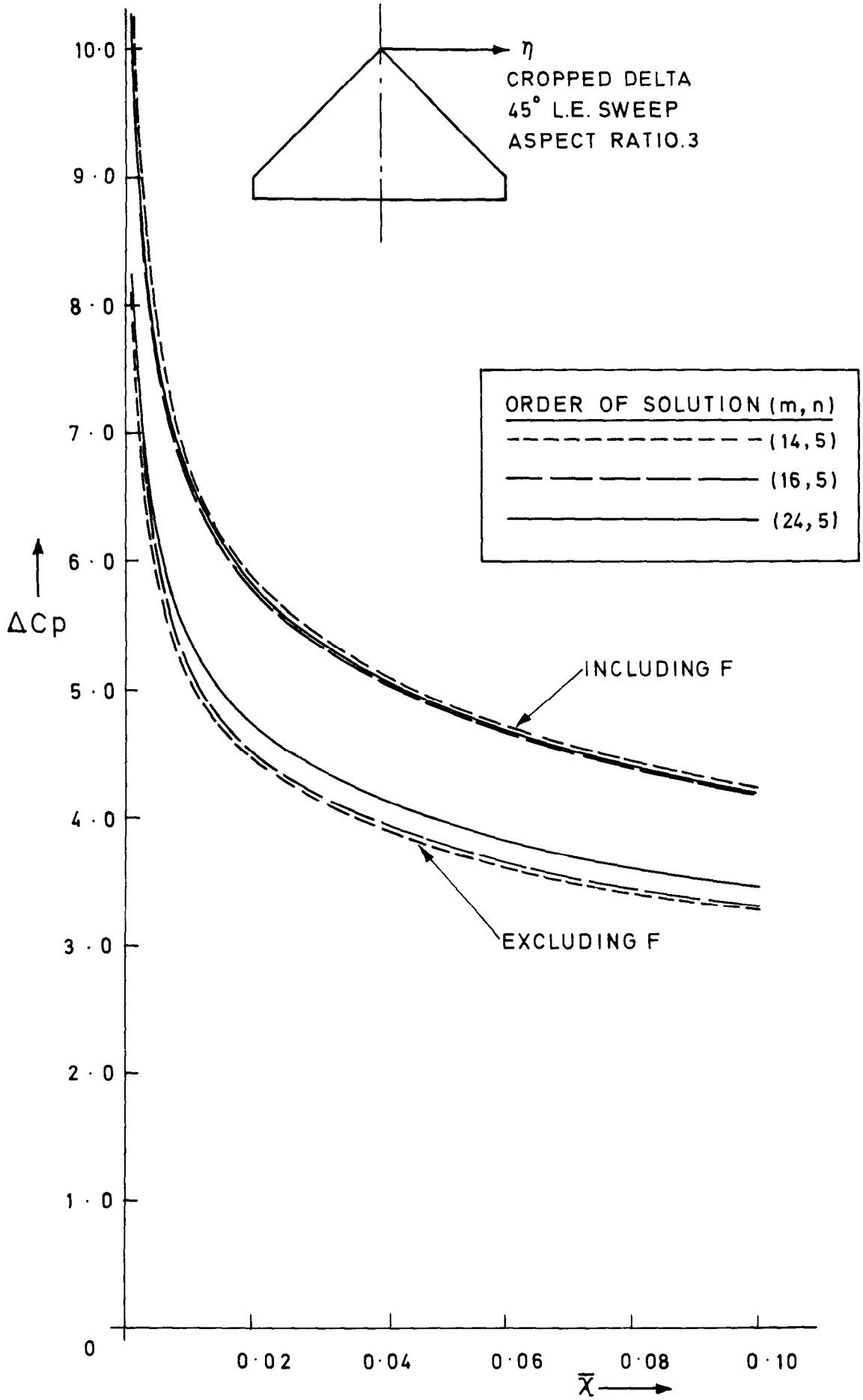

FIG.9. COMPARISON OF CONVERGENCE ΔCp AT η=0 WITH INCREASING SPANWISE TERMS

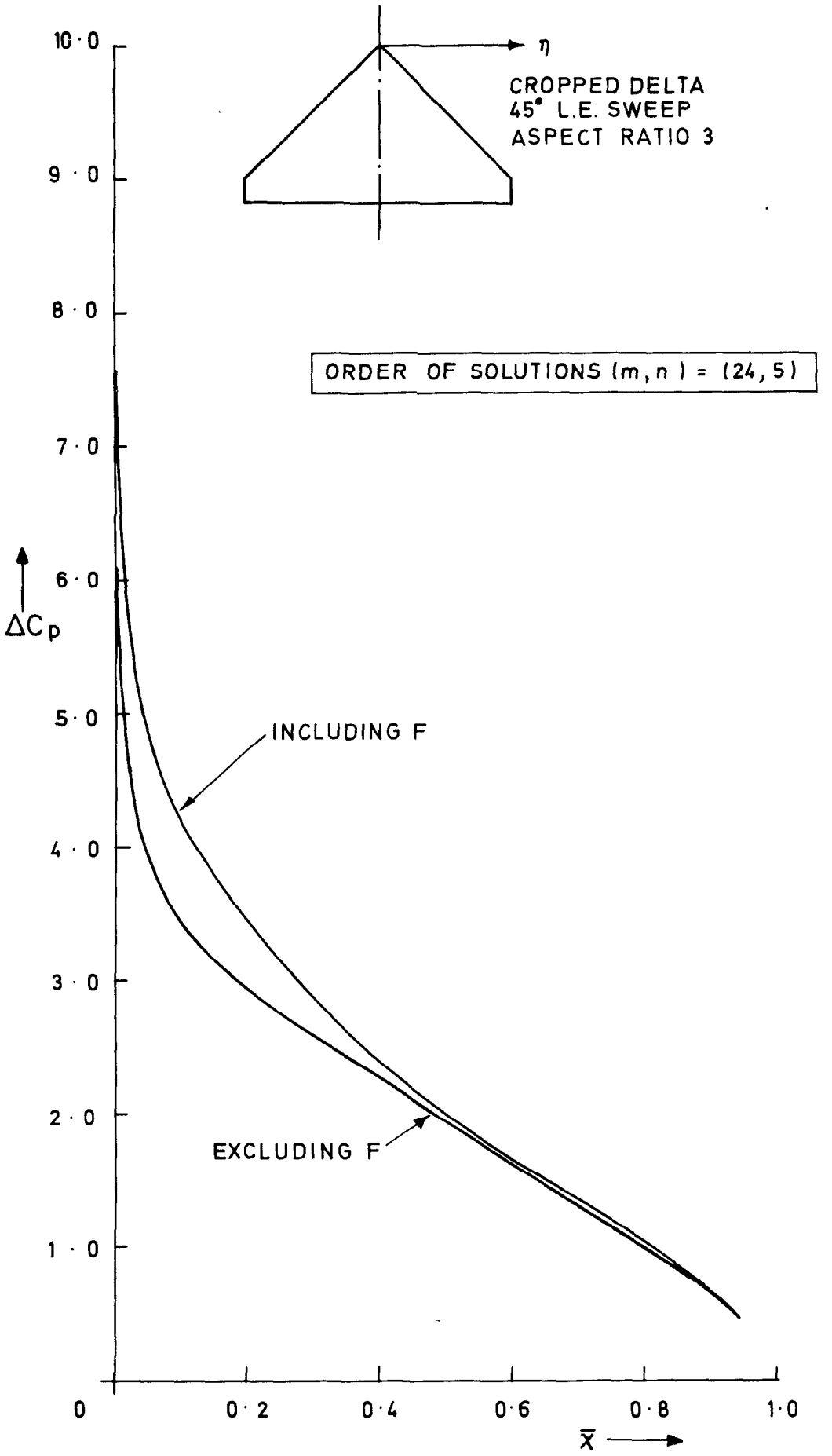

FIG.10. COMPARISON OF ΔCp DISTRIBUTION AT $\eta=0$

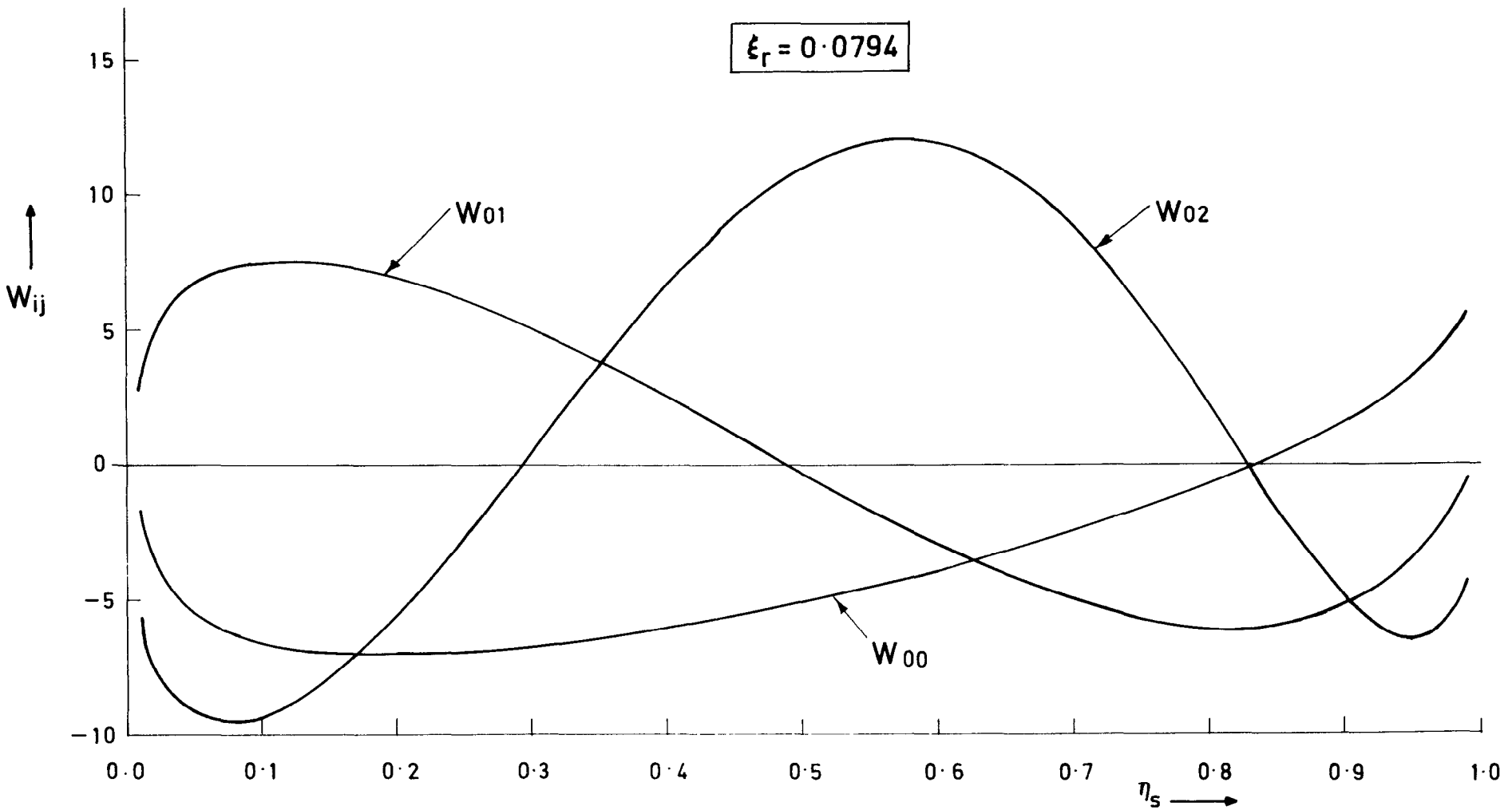

FIG. 11 VARIATION OF SPANWISE DOWNWASH MODES (EXCLUDING F)

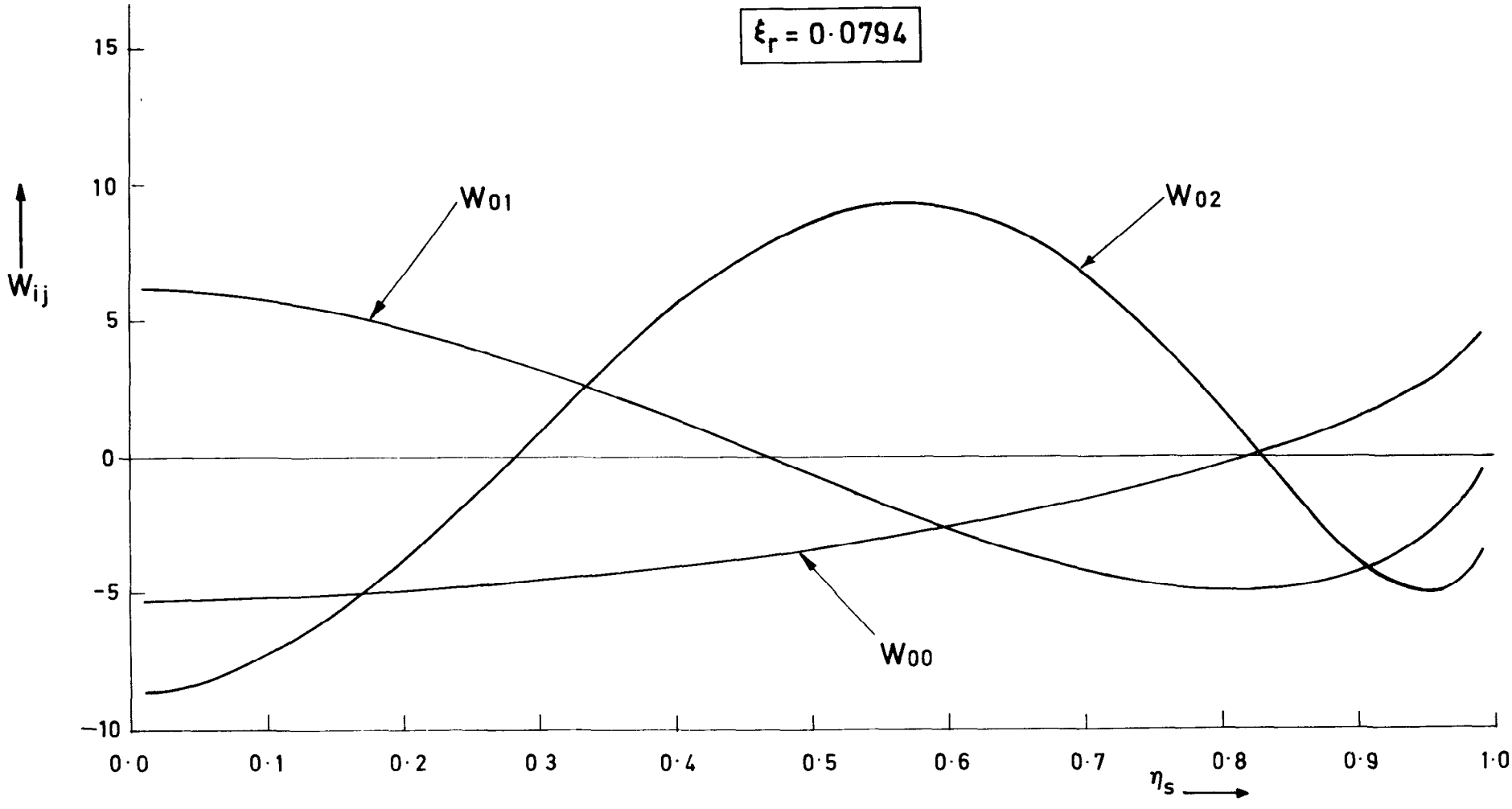

FIG. 12. VARIATION OF SPANWISE DOWNWASH MODES (INCLUDING F)

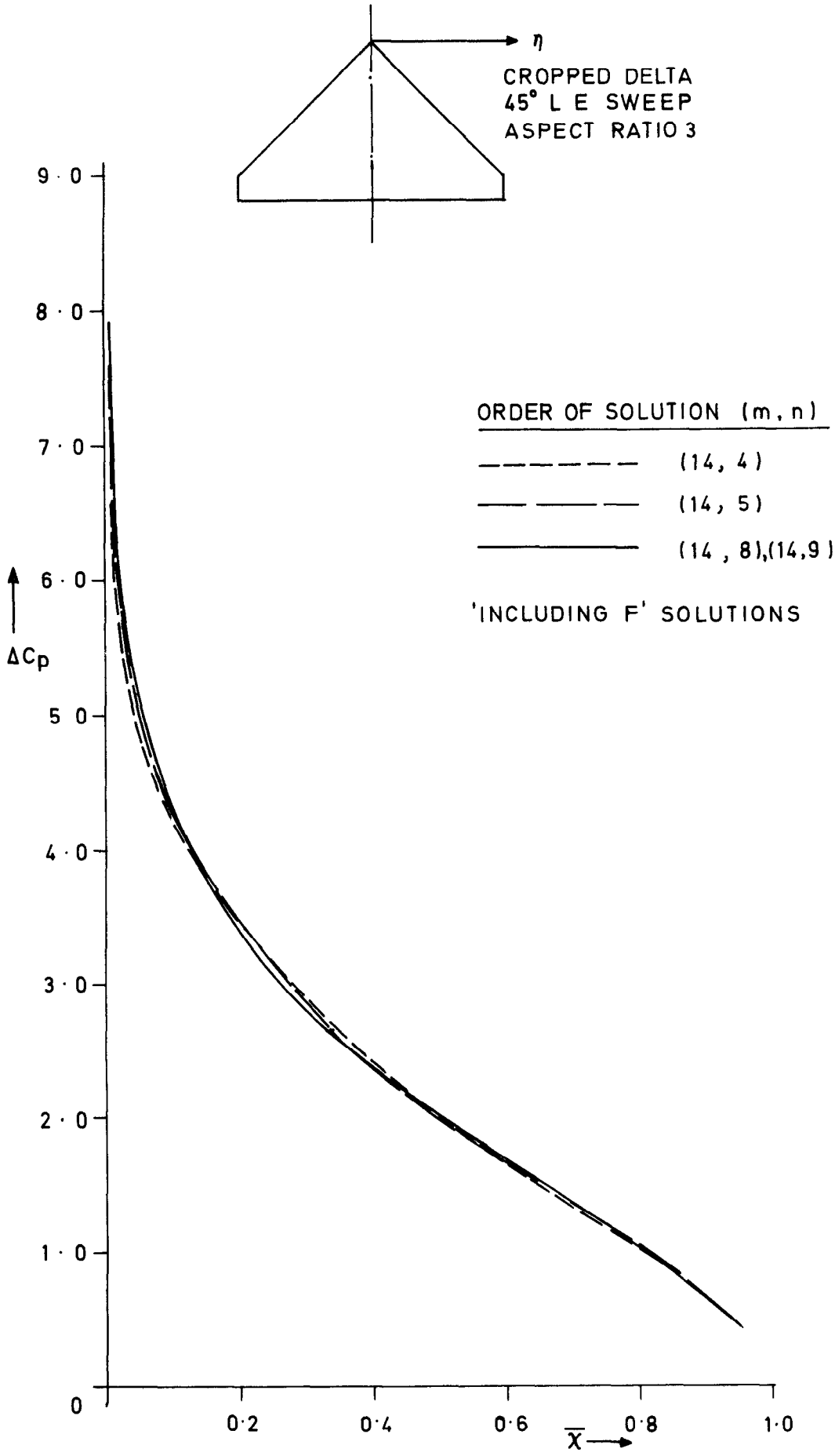

FIG.13. CONVERGENCE OF ΔCp AT η=0 WITH INCREASING CHORDWISE TERMS

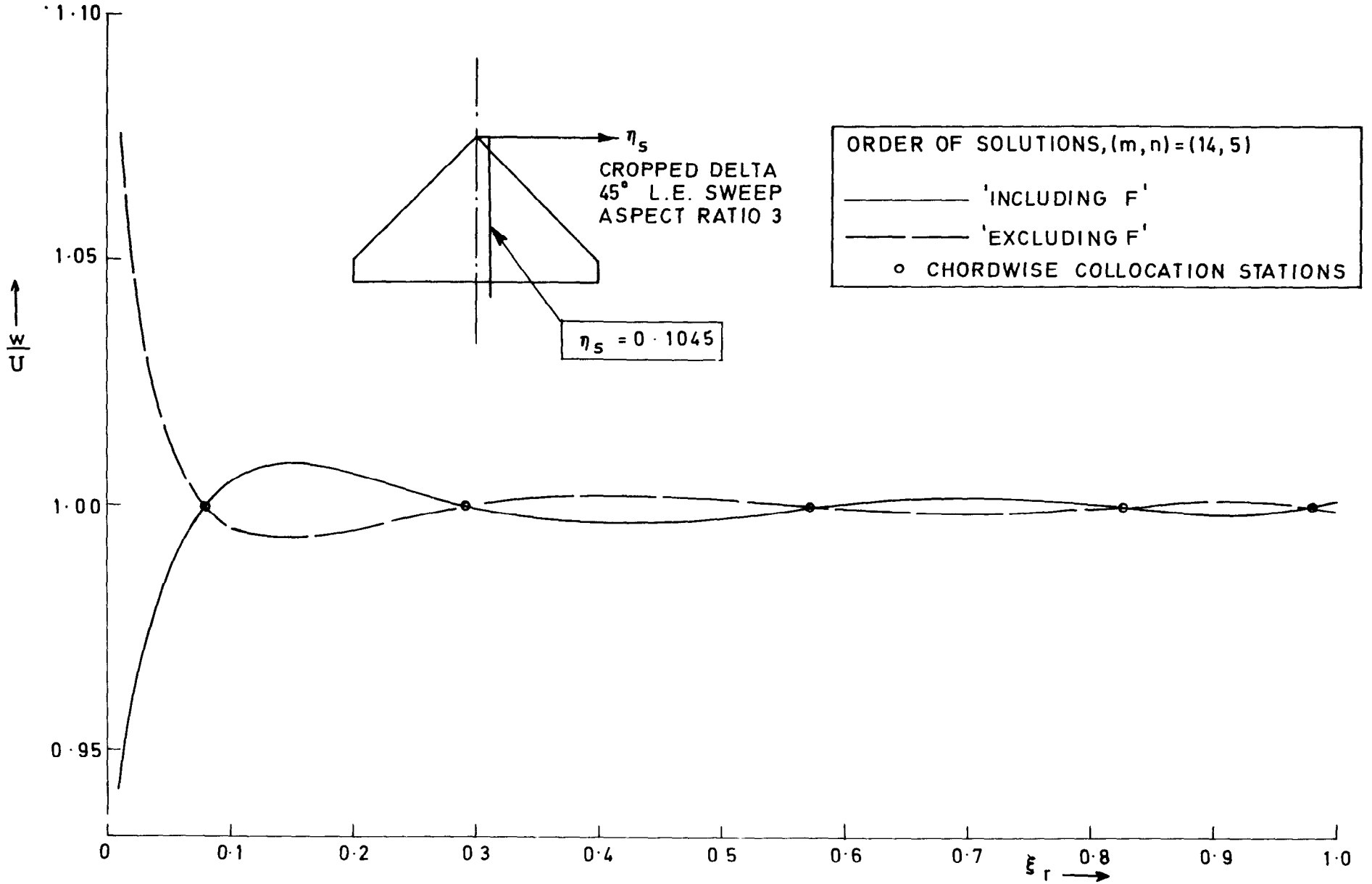

FIG. 14. CHORDWISE DOWNWASH INTERPOLATION AT SPANWISE COLLOCATION STATION, η_s=0·1045

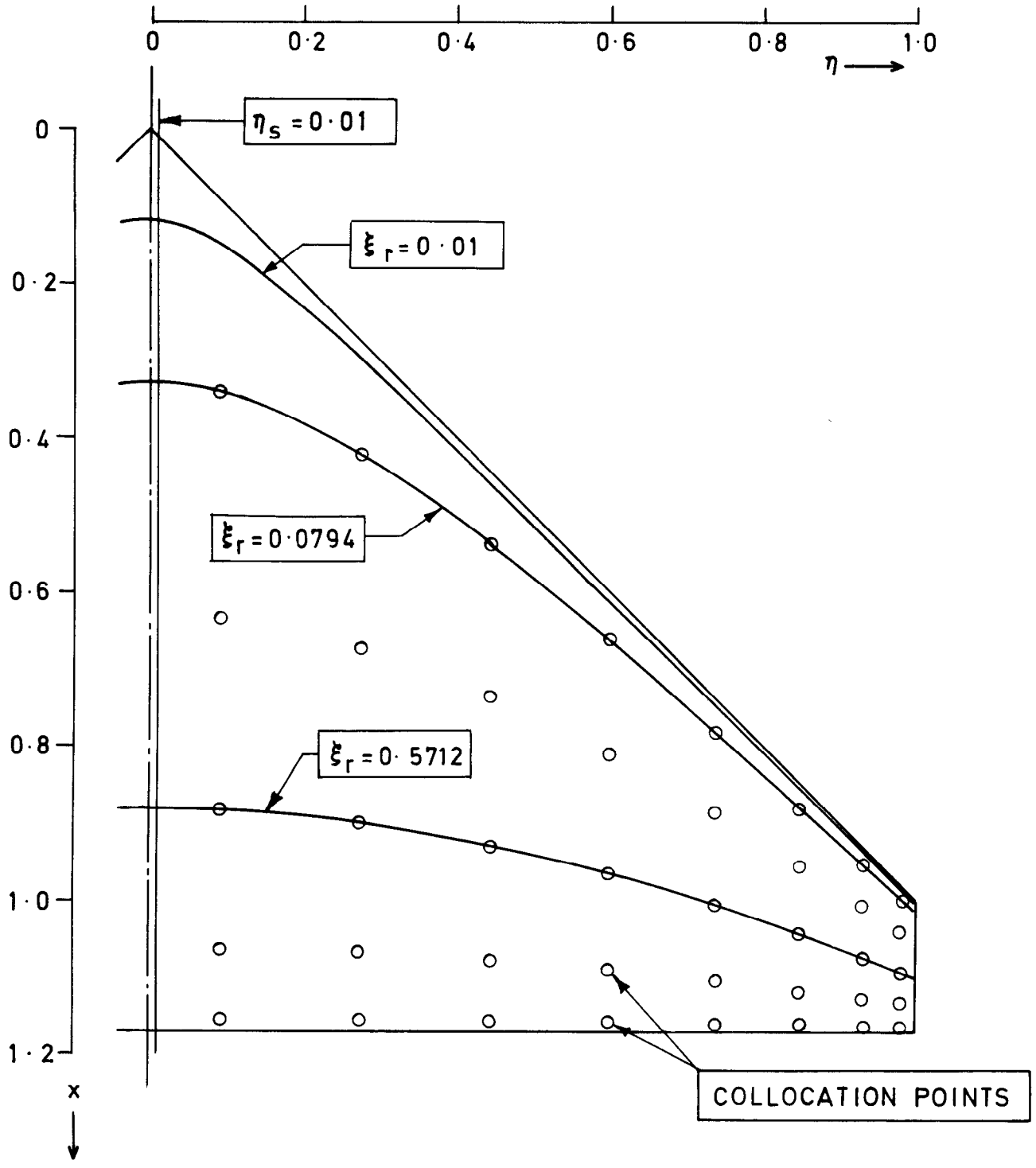

FIG. 15. CROPPED DELTA. COLLOCATION DISTRIBUTION AND DOWNWASH INTERPOLATION LINES FOR SOLUTIONS WITH (m, n) = (16, 5).

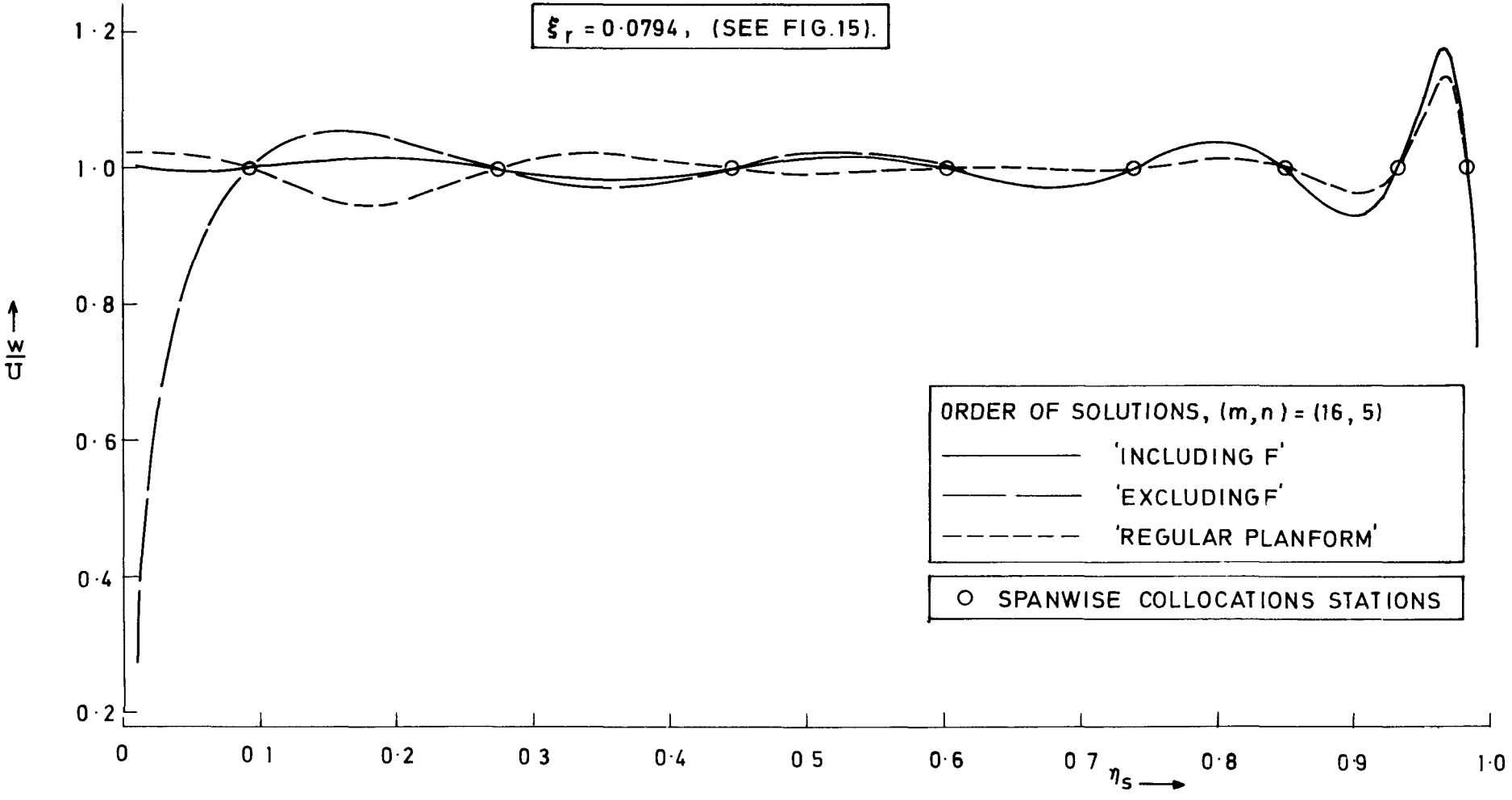

FIG. 16. SPANWISE DOWNWASH INTERPOLATION AT CHORDWISE COLLOCATION STATION, ξ_r = 0·0794

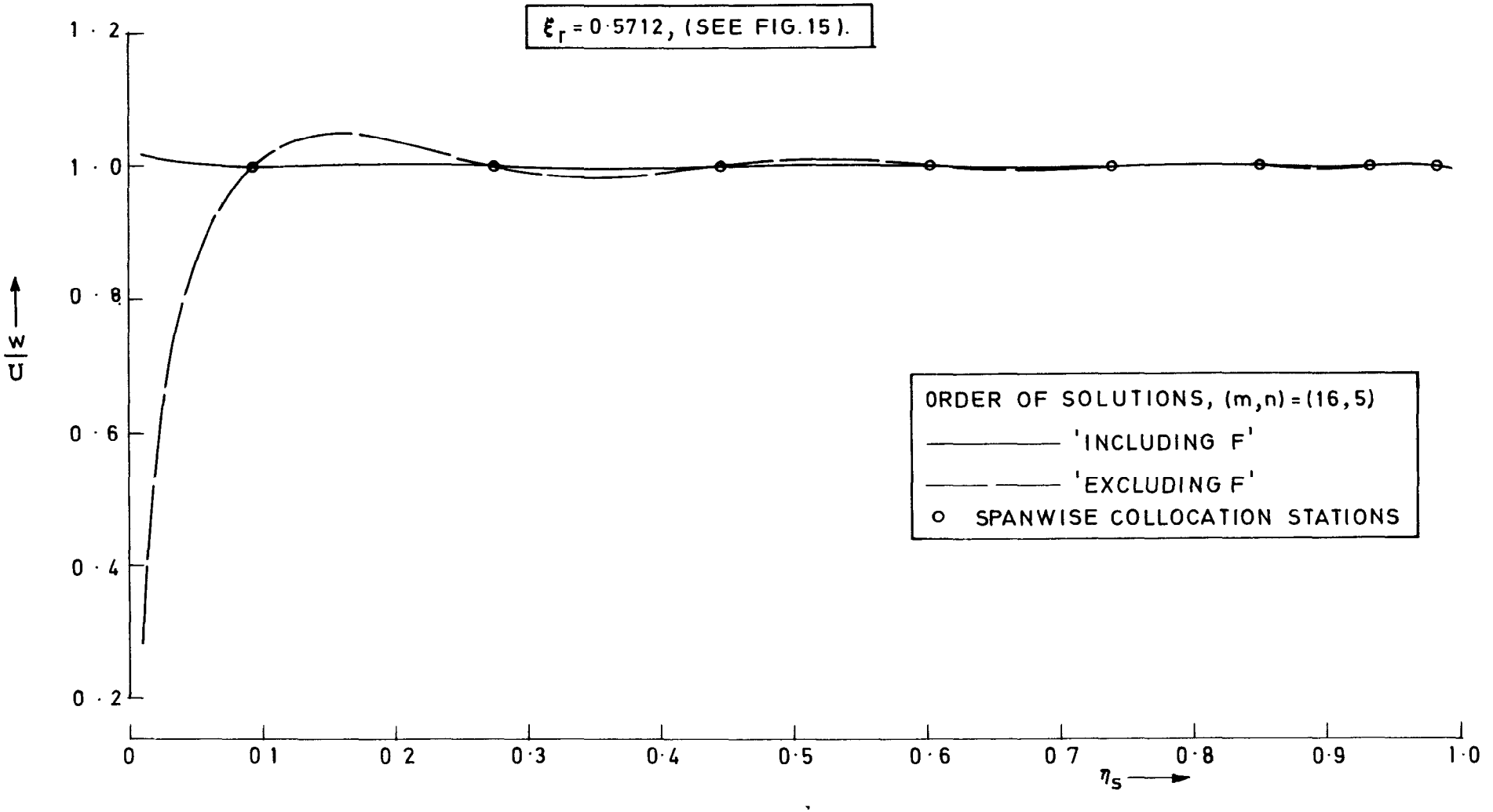

FIG.17. SPANWISE DOWNWASH INTERPOLATION AT CHORDWISE COLLOCATION STATION, $\xi_r = 0{\cdot}5712$

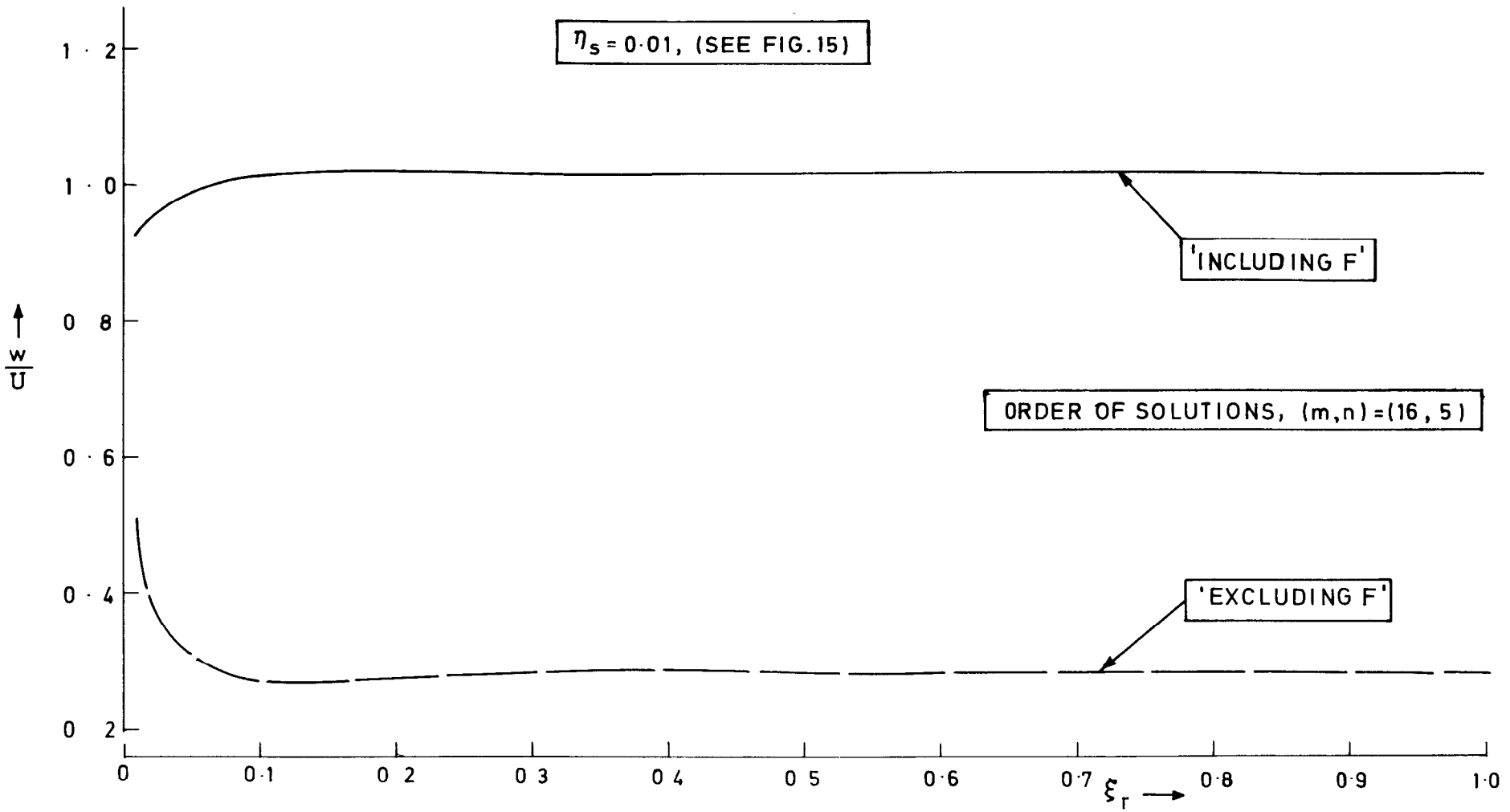

FIG.18. CHORDWISE DOWNWASH INTERPOLATION AT $\eta_s = 0{\cdot}01$

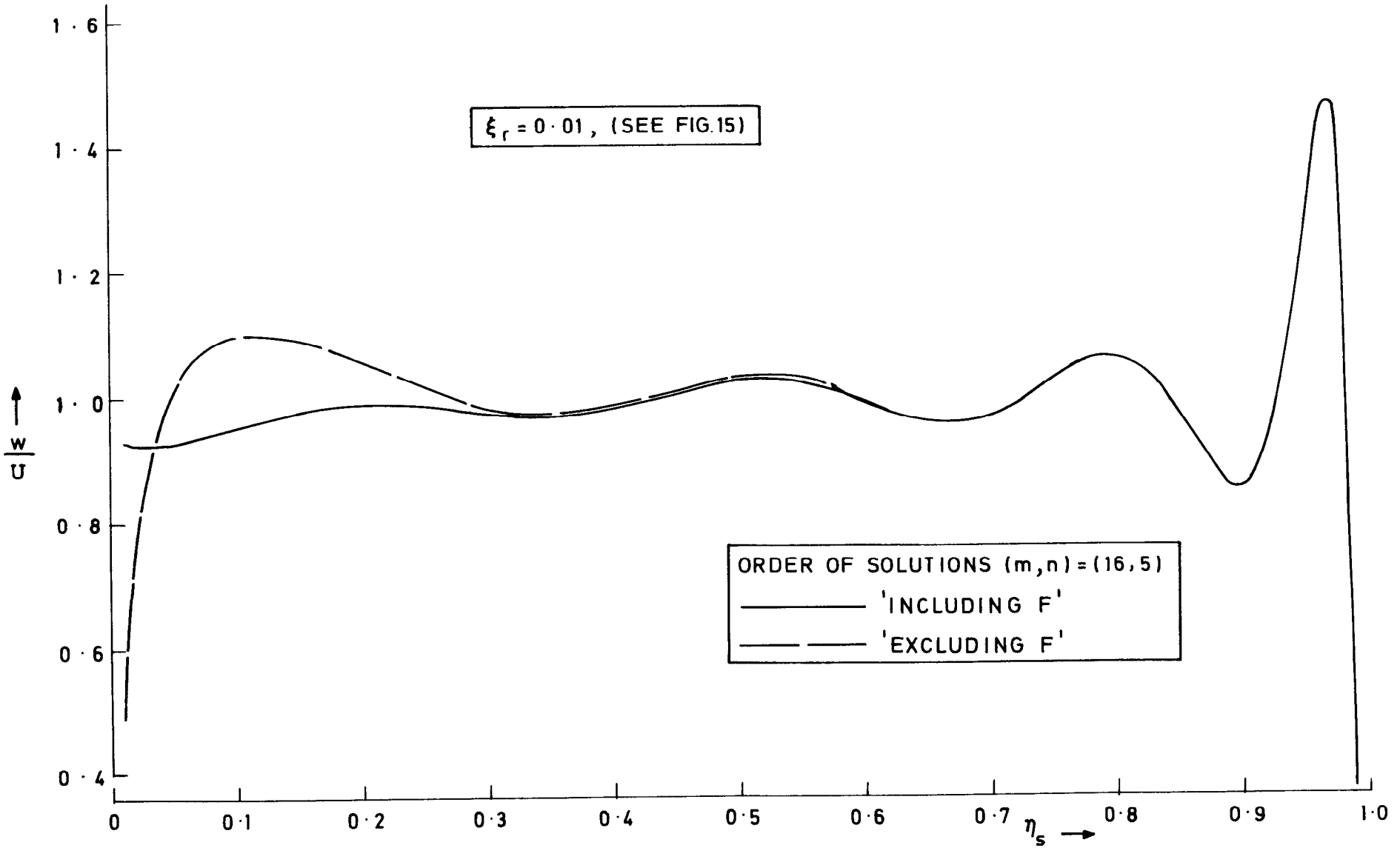

FIG.19. SPANWISE DOWNWASH INTERPOLATION AT $\xi_r = 0 \cdot 01$

ARC CP No.1323
October 1972
Hewitt, B.L. and Kellaway, W.

DEVELOPMENTS IN THE LIFTING SURFACE THEORY TREATMENT OF SYMMETRIC PLANFORMS WITH A LEADING EDGE CRANK IN SUBSONIC FLOW

An attempt has been made to develop a subsonic lifting surface theory method capable of calculating convergent loading solutions for symmetric planforms with a leading edge crank. This document traces the time history of thought and method development at B.A.C. (Military Aircraft Division) which connects the successful treatments of regular and cropped delta type planforms that are reported in References 1 and 13, respectively. Finally, some mention is made of possible future generalisations of the basic cranked planform method.

ARC CP No.1323
October 1972
Hewitt, B.L. and Kellaway, W.

DEVELOPMENTS IN THE LIFTING SURFACE THEORY TREATMENT OF SYMMETRIC PLANFORMS WITH A LEADING EDGE CRANK IN SUBSONIC FLOW

An attempt has been made to develop a subsonic lifting surface theory method capable of calculating convergent loading solutions for symmetric planforms with a leading edge crank. This document traces the time history of thought and method development at B.A.C. (Military Aircraft Division) which connects the successful treatments of regular and cropped delta type planforms that are reported in References 1 and 13, respectively. Finally, some mention is made of possible future generalisations of the basic cranked planform method.

ARC CP No.1323
October 1972
Hewitt, B.L. and Kellaway, W.

DEVELOPMENTS IN THE LIFTING SURFACE THEORY TREATMENT OF SYMMETRIC PLANFORMS WITH A LEADING EDGE CRANK IN SUBSONIC FLOW

An attempt has been made to develop a subsonic lifting surface theory method capable of calculating convergent loading solutions for symmetric planforms with a leading edge crank. This document traces the time history of thought and method development at B.A.C. (Military Aircraft Division) which connects the successful treatments of regular and cropped delta type planforms that are reported in References 1 and 13, respectively. Finally, some mention is made of possible future generalisations of the basic cranked planform method.

DETACHABLE ABSTRACT CARDS

HER MAJESTY'S STATIONERY OFFICE

Government Bookshops

49 High Holborn, London WC1V 6HB
13a Castle Street, Edinburgh EH2 3AR
41 The Hayes, Cardiff CF1 1JW
Brazennose Street, Manchester M60 8AS
Southey House, Wine Street, Bristol BS1 2BQ
258 Broad Street, Birmingham B1 2HE
80 Chichester Street, Belfast BT1 4JY

Government publications are also available through booksellers

C.P. No. 1323

ISBN O 11 4709335